NAT'L INST. OF STAND & TECH R.I.C.
A11104 556427
NIST
PUBLICATIONS

NISTIR 5516

Method of Predicting Smoke Movement in Atria With Application to Smoke Management

John H. Klote

Building and Fire Research Laboratory
Gaithersburg, Maryland 20899

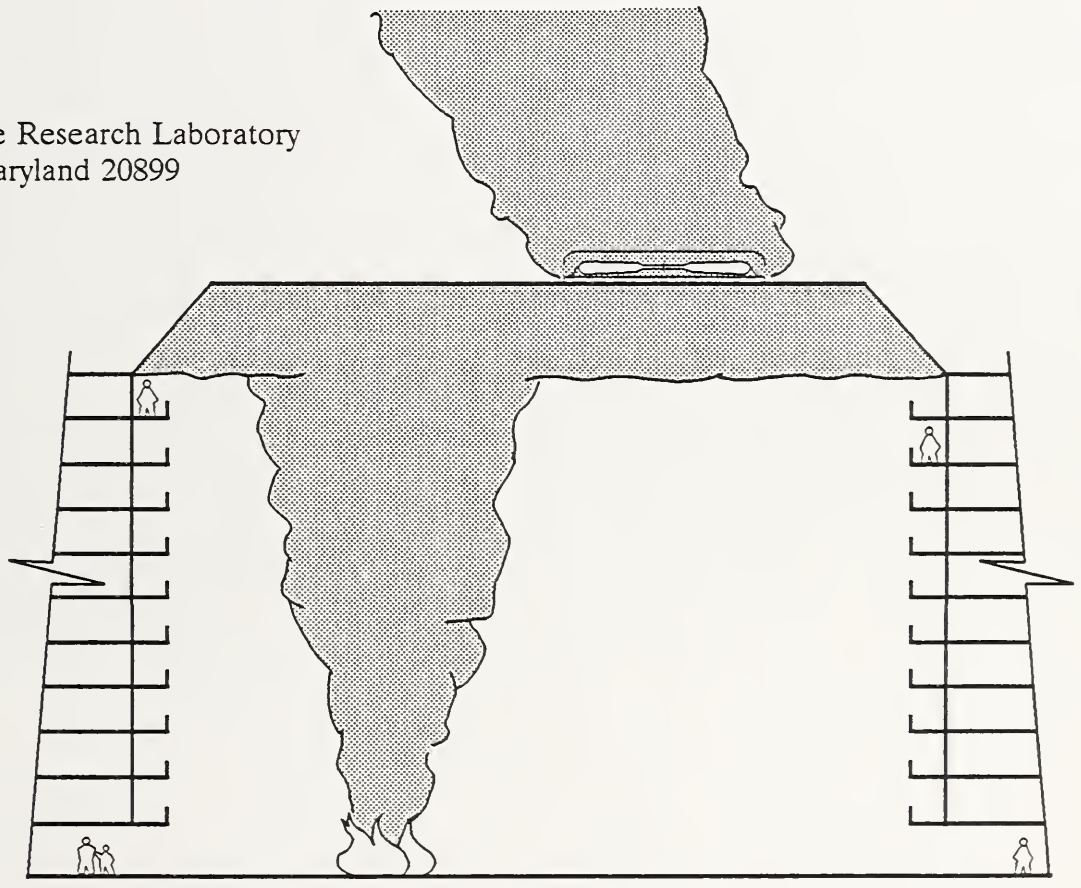

NIST

d States Department of Commerce
ıology Administration
nal Institute of Standards and Technology

QC
100
.U56
NO.5516
19994

NISTIR 5516

Method of Predicting Smoke Movement in Atria With Application to Smoke Management

John H. Klote

November 1994

Building and Fire Research Laboratory
National Institute of Standards and Technology
Gaithersburg, Maryland 20899

U.S. Department of Commerce
Ronald H. Brown, *Secretary*
Technology Administration
Mary L. Good, *Under Secretary for Technology*
National Institute of Standards and Technology
Arati Prabhakar, Director

Table of Contents

List of Tables v

List of Figures vi

1. Introduction 1

2. Design Fires 2
    2.1 Steady Fires 2
    2.2 Unsteady Fires 3

3. Zone Fire Model Concept 5

4. Fire Plumes 6
    4.1 Mass Flow With Virtual Origin Correction 8
    4.2 Virtual Origin 8
    4.3 Average Plume Temperature 9
    4.4 Volumetric Flow 10
    4.5 Plume Centerline Temperature 10
    4.6 Air and Plume Gas Density 11
    4.7 Plume Diameter 11
    4.8 Flame Height 12
    4.9 Simple Mass Flow and Flame Height Equations 12
    4.10 Discussion of Simple Equations 13

5. Approaches for Smoke Management 17
    5.1 Filling by a Steady Fire 18
    5.2 Filling by an Unsteady Fire 19
    5.3 Steady Clear Height With Upper Layer Exhaust 20

6. Pre-Stratification and Detection 22

7. Make-Up Air 23

8. Separated Spaces 23

9. Communicating Spaces 24
    9.1 Other Plumes 24
    9.2 Airflow for a Communicating Space Fire 24
    9.3 Airflow for an Atrium Fire 26

10. Commissioning and Acceptance Testing 26
    10.1 Fire Tests 27
    10.2 Performance Tests Without a Fire 27

10.3 Chemical Smoke Tracer Tests 28
10.4 Caution About Chemical Smoke 28

11. Summary and Conclusions 28

12. Acknowledgements 29

13. Nomenclature 30

14. References 31

Appendix A Bibliography 35

Appendix B Unit Systems and Physical Data 41

Appendix C ASMET Description 45

Appendix D ASMET Users Guide 49

Appendix E ASET-C: A Room Fire Program for Personal Computers 57

Appendix F Physical Modeling 67

Appendix G Computational Fluid Dynamics 76

Appendix H Considerations of the Steady Plume 87

List of Tables

Table 1. Steady design fire sizes for atria 3
Table 2. Typical fire growth constants 3
Table 3. Heat release density of some materials 15
Table 4. Deviations of mass flow due to omitting the virtual origin correction 16

List of Figures

Figure 1. Fire growth (a) typical curve, and (b) idealized parabolic curve 4
Figure 2. Relation of t-squared fires to some fire tests (adapted from Nelson 1987) 4
Figure 3. Fire curves with fast t-square growth up to a steady size of 2, 5 and 25 MW 5
Figure 4. Room fire (a) sketch and (b) zone model idealization 6
Figure 5. Atrium fire (a) sketch and (b) zone model idealization 7
Figure 6. Fire plume and idealized model of axisymetric, point source plume 7
Figure 7. Control volume for idealized plume 9
Figure 8. The effect of heat release density, q, on the elevation of the virtual origin 13
Figure 9. Comparison of mass flow predictions with and without correction for virtual origin for a heat release density of 400 kW/m^2 (35 Btu/s ft^2) 13
Figure 10. Comparison of mass flow predictions with and without correction for virtual origin for a heat release density of 10,000 kW/m^2 (880 Btu/s ft^2) 14
Figure 11. Comparison of predicted flame heights to the approximate equation (dashed line) 14
Figure 12. Smoke exhaust to maintain constant clear height 17
Figure 13. Smoke layer interface 18
Figure 14. Pre-stratified layer of hot air under atrium ceiling and the resulting temperature profile 22
Figure 15. Smoke filling a pre-stratified atrium 23
Figure 16. Average plume temperature calculated from equations (6) and (14) 23
Figure 17. Beam detectors used for activation of atrium smoke management system 24

Method of Predicting Smoke Movement in Atria With Application to Smoke Management

John H. Klote

1. Introduction

In recent years, the atrium building has become commonplace. Other large open spaces include enclosed shopping malls, arcades, sports arenas, exhibition halls and airplane hangers. The methods of this paper also apply to these spaces. For simplicity, the term atrium is used in this paper in a generic sense to mean any of these large spaces. The traditional approach to fire protection by compartmentation is not applicable to these large volume spaces.

The ability of sprinklers to suppress fires in spaces with ceilings higher than 11 to 15 m (35 to 50 ft) is limited (Degenkolb 1975, 1983). Because the temperature of smoke decreases as it rises (due to entrainment of ambient air), smoke may not be hot enough to activate sprinklers mounted under the ceiling of an atrium. Even if such sprinklers activate, the delay can allow fire growth to an extent beyond the suppression ability of ordinary sprinklers. Some studies have been done concerning prediction of smoke movement and temperature in tall spaces (Notarianni and Davis 1993; Walton and Notarianni 1993). Considering the limitations of compartmentation and sprinklers for atriums, it is not surprising that the fire protection community is concerned about atrium smoke management.

This paper presents information that can be used for predicting smoke movement for design of atrium smoke management systems. NFPA 92B (1991) and the smoke control design book by Klote and Milke (1992) define smoke as the airborne solid and liquid particulates and gases evolved when a material undergoes pyrolysis or combustion, together with the quantity of air that is entrained or otherwise mixed into the mass. In recent years, approaches to smoke management in atria have been introduced into codes and engineering guides (BOCA 1993; UBC 1993; NFPA 92B 1991; Klote and Milke 1992; Hansel and Morgan 1994). While these basic approaches differ in many respects, they all have the zone fire model concept as a common foundation and consist of a collection of algebraic equations intended for design calculation. For simplicity, discussion of the basic approaches is limited to those of NFPA 92B. However, much of this applies to the other approaches as well.

This paper explains the physical concepts behind NFPA 92B including system limitations. The conservative nature of this approach is investigated, and the unique design challenge of atrium smoke detection is discussed. The application of zone computer fire models to atrium design is addressed. This paper also presents a computer program entitled *Atria Smoke Management Engineering Tools* (ASMET) that consists of a set of equations that may be of help for conventional applications. Appendices C and D describe ASMET including brief user instructions. However, the program is menu driven and readers familiar with computers will probably be able to use it without aid of these instructions.

The basic calculation methods of this paper are not applicable when the design exceeds the range of applicability of the equations presented or when obstructions in an atrium do not allow flow. For these situations, there may be benefit to computational fluid dynamic (CFD) modeling or physical modeling. CFD modeling and physical modeling provide greater information than usual design methods but require specialized and advanced engineering training. Introductory information about these topics is provided in Appendices F and G.

2. Design Fires

The design fire has a major impact on the atrium smoke management system. The fire size is expressed in terms of the rate of heat release. Fire growth is the rate of change of the heat release rate and is sometimes expressed as a growth constant that identifies the time required for the fire to attain a particular rate of heat release. Designs may be based on either steady fires or unsteady fires.

2.1 Steady Fires

It is the nature of fires to be unsteady, but the steady fire is a very useful idealization. Steady fires have a constant heat release rate. In many applications, use of a steady design fire leads to straight-forward and conservative design.

Morgan (1979) suggests a typical rate of heat release per unit floor area for mercantile occupancies of 500 kW/m^2 (44 $Btu/s\ ft^2$). Fang and Breese (1980) determined about the same rate of heat release for residential occupancies. Morgan and Hansell (1987) and Law 1982 suggest a heat release rate per unit floor area for office buildings of 225 kW/m^2 (20 $Btu/s\ ft^2$).

In many atria, the fuel loading is severely restricted with the intent of restricting fire size. Such atria are characterized by interior finishes of metal, brick, stone or gypsum board and furnished with objects made of similar materials plus plants. Even for such a *fuel restricted* atrium, there are many combustible objects that are in the atrium for short periods. Packing materials, Christmas decorations, displays, construction materials, and furniture being moved into another part of the building are a few examples of *transient fuels*. For this paper, a heat release rate per floor area of 225 kW/m^2 (20 $Btu/s\ ft^2$) will be used for a restricted fuel atria, and 500 kW/m^2 (44 $Btu/s\ ft^2$) will be used for atria with furniture, wood or other combustible materials.

Transient fuels must not be overlooked when selecting a design fire. The approach suggested by Klote and Milke (1992) to incorporating transient fuels in a design fire is to consider the fire occurring over 9.3 m^2 (100 ft^2) of floor space. This results in a design fire of 2100 kW (2000 Btu/s) for restricted fuel atria. If a fire occurred over 9.3 m^2 (100 ft^2) of an atria with combustibles, a design fire of 4600 kW (4400 Btu/s) would result. However, the area involved in fire may be much greater, and determination of it involves flame spread considerations (NFPA 92B 1991, Klote and Milke 1992). A large atrium fire of 25,000 kW would involve an area of 50 m^2 (540 ft^2) at 500 kW/m^2 (44 $Btu/s\ ft^2$). For this paper, discussion of steady design fires will be focused on those listed in table 1.

Table 1. Steady design fire sizes for atria

	kW	(Btu/s)
Minimum fire for fuel restricted atrium	2,000	(1,900)
Minimum fire for atrium with combustibles	5,000	(4,700)
Large fire	25,000	(24,000)

Table 2. Typical fire growth constants

	Growth Constant		Growth Time
T-Squared Fires	a (kW/s^2)	a (Btu/s^3)	t_g (s)
Slow‡	0.002931	0.002778	600
Medium‡	0.01127	0.01111	300
Fast‡	0.04689	0.04444	150
Ultra Fast§	0.1878	0.1778	75

‡Constants for these fire growth types based on data from NFPA 204 (1991) and NFPA 92B (1991).
§Constants for the ultra fast fire based on data from Nelson (1987).

2.2 Unsteady Fires

Fires frequently proceed through an incubation period of slow and uneven growth followed by a period of established growth as illustrated in figure 1 (a). Figure 1 (b) shows the established growth is often represented by an idealized parabolic equation (Heskestad 1984).

$$Q = a(t - t_o)^2 \tag{1}$$

where
Q = heat release rate of fire, kW (Btu/s);
a = fire growth coefficient, kW/s^2 (Btu/s^3);
t = time after ignition, s;
t_o = effective ignition time, s.

It is generally recognized that consideration of the incubation period is not necessary for design of atrium smoke control systems, and equation (1) can be expressed as

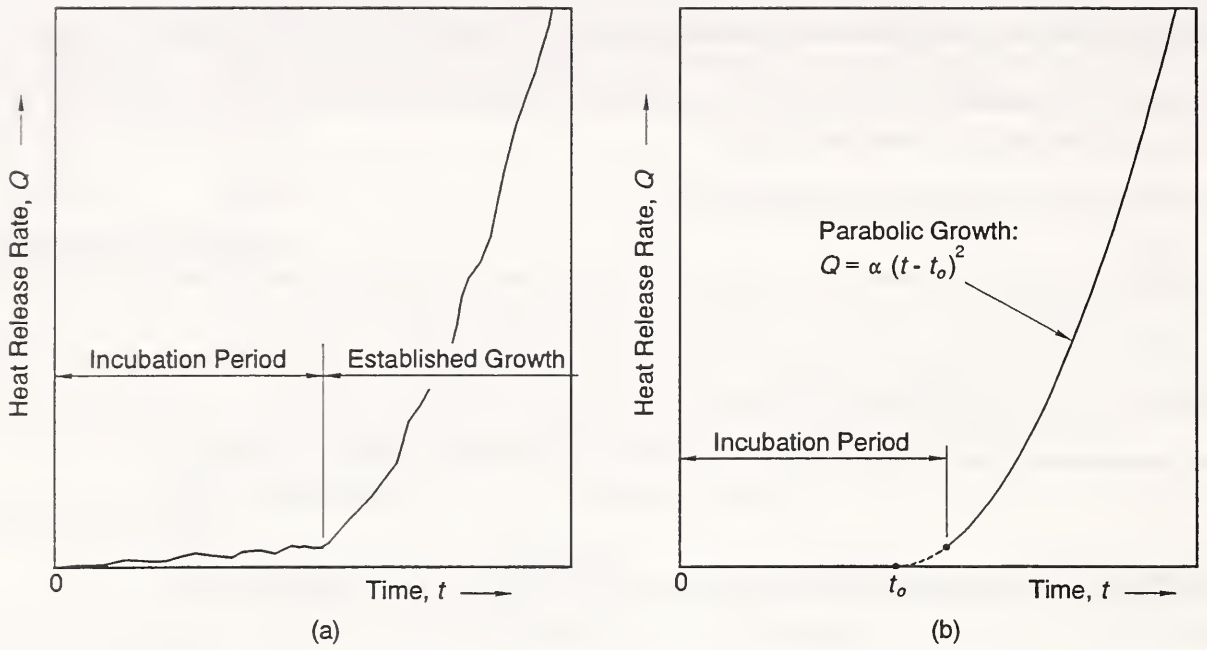

Figure 1. Fire growth (a) typical curve, and (b) idealized parabolic curve

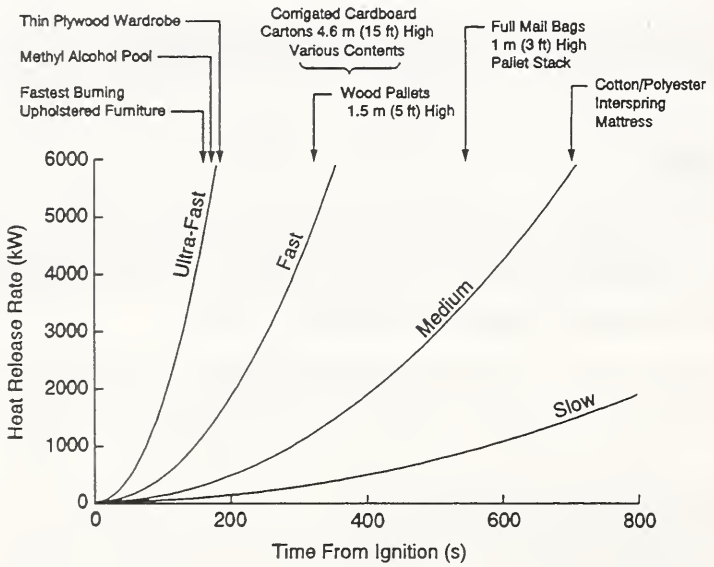

Figure 2. Relation of t-squared fires to some fire tests (adapted from Nelson 1987)

$$Q = a t^2 \qquad (2)$$

where t is the time after effective ignition, and fires following equation (2) are called *t-squared fires*. NFPA 92B (1991) makes extensive use of the growth time concept, where the growth time, t_g, is the time after effective ignition for the fire to grow to 1055 kW (1000 Btu/s). Table 2 lists values of a and t_g for some general fire types, and the corresponding fire growths are shown on figure 2.

Fire growth may be approximated by the t-squared curve for some time. Because of the action of a suppression system, limitations of fuel, or limitations of combustion air; t-squared fire growth eventually must stop. Generally the action of a suppression system results in a decrease in the heat release rate (Madrzykowski 1991). However, limitations of fuel and of combustion air can result in a nearly constant rate of heat release following a t-squared fire growth. Because atria are large spaces, the growth of fires in atria is usually not restricted by lack of combustion air. Figure 3 is illustrates t-squared fire growth followed by a constant heat release rate.

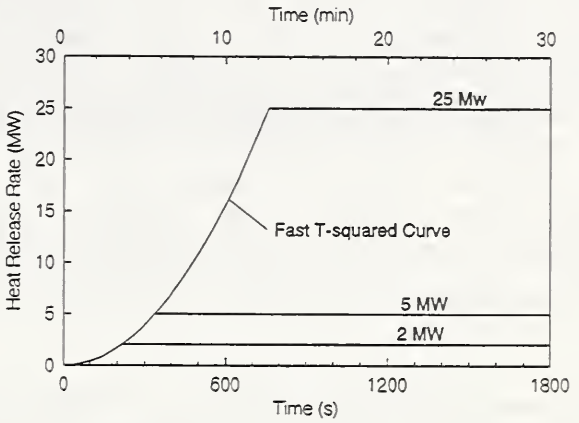

Figure 3. Fire curves with fast t-square growth up to a steady size of 2, 5 and 25 MW

3. Zone Fire Model Concept

The basic approach to smoke control design calculation in codes is based on the zone fire model concept. Also this concept has been applied to several computer models. These computer models include the Harvard Code (Mitler and Emmons 1981), ASET (Cooper 1985), the BRI Model (Tanaka 1983), CCFM (Cooper and Forney 1990), and CFAST (Peacock et al. 1993). The University of Maryland has made modifications to CCFM specifically for atrium smoke management design (Milke and Mower 1994). CFAST has an approach to account for mass being added to the upper layer when the plume temperature is lower than that of the smoke layer. While each of these models has unique features, they all share the same basic two zone model concept.

This section is an overview of zone fire modeling, but for more information about zone models readers are referred to Bukowski (1991), Friedman (1992), Jones (1983), Mitler and Rockett (1986), Mitler (1984) and Quintiere (1989). Zone models have proven utility for many fire protection applications including hazard analysis (Peacock et al. 1991; Bukowski et al. 1991). The ASET-B model (Walton 1985) is a simple model that is a good starting point for people to learn about zone models. As a convenience to the reader, an enhanced version of ASET-B, called ASET-C, is included in ASMET, and this model is discussed in detail in Appendix E.

Because zone models were originally developed for room fires, this discussion will start with room fires. In a room fire, hot gases rise above the fire forming a plume. As the plume rises, it entrains air from the room so that the diameter and mass flow rate of the plume increase with elevation. Accordingly, the plume temperature decreases with elevation. The fire gases from the plume flow up to the ceiling and form a hot stratified layer under the ceiling. The hot gases can flow through openings in walls to other spaces, and such flow is referred to as a doorjet. The doorjet is similar to a plume in that air is entrained and the mass flow rate and cross-sectional area of the jet increase with elevation, and the jet temperature decreases with elevation. The difference is that the doorjet is flowing through an opening in a wall. Figure 4 (a) is a sketch of a room fire.

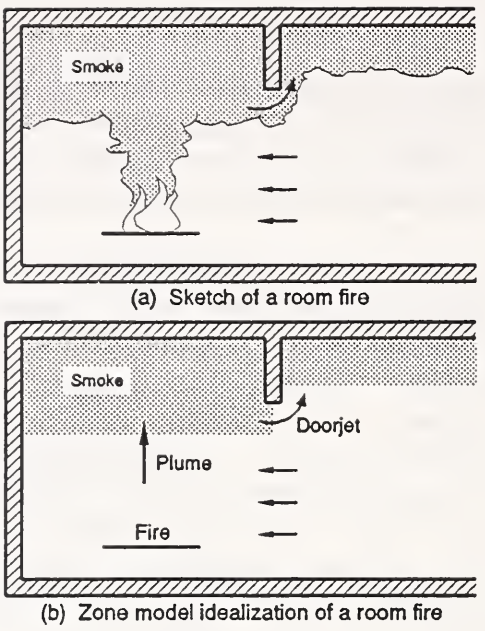

Figure 4. Room fire (a) sketch and (b) zone model idealization

The concept of zone modeling is an idealization of the room fire conditions as illustrated in figure 4 (b). For this idealization the temperature of the hot upper layer of the room is uniform, and the temperature of the lower layer of this room is also uniform. The height of the discontinuity between these layers is the same everywhere. The dynamic effects on pressure are considered negligible, so that the pressures are treated as hydrostatic. Other properties are considered uniform for each layer. Algebraic equations are used to calculate the mass flows due to plumes and doorjets.

Many zone computer models allow exhaust from the upper layer, and this capability is essential for simulation of atrium smoke exhaust systems. Many of the computer zone models estimate heat transfer by methods ranging from a simple allowance as a fraction of the heat released by the fire to complicated simulation including the effects of conduction, convection and radiation. Zone model application to an atrium fire is illustrated in figures 5 (a) and (b).

4. Fire Plumes

The plumes above fires that are of interest in this paper pulsate and are formed of many eddies. Morton, Taylor and Turner (1956) developed a classic analysis of the time averaged flow of plumes. They considered the plume to be coming from a point source (or a line source). For a height above the plume source, they considered the air entrained at the plume edge to be proportional to some characteristic velocity of the plume at that height. The variations of density in the plume were considered small compared to ambient density. The profiles of mean vertical velocity and mean buoyancy force in the horizontal sections were considered to be of similar form at all heights. Figure 6 is an illustration of a plume next to the idealized model of a plume.

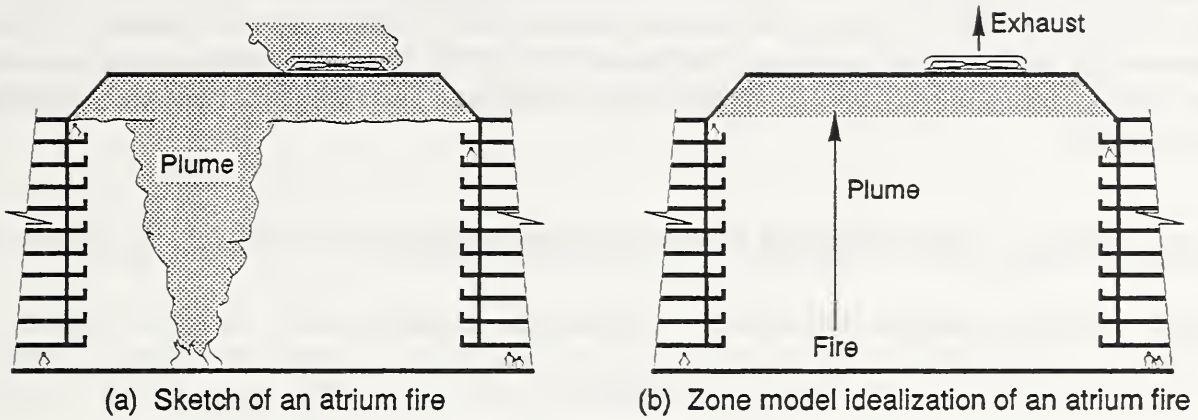

Figure 5. Atrium fire (a) sketch and (b) zone model idealization

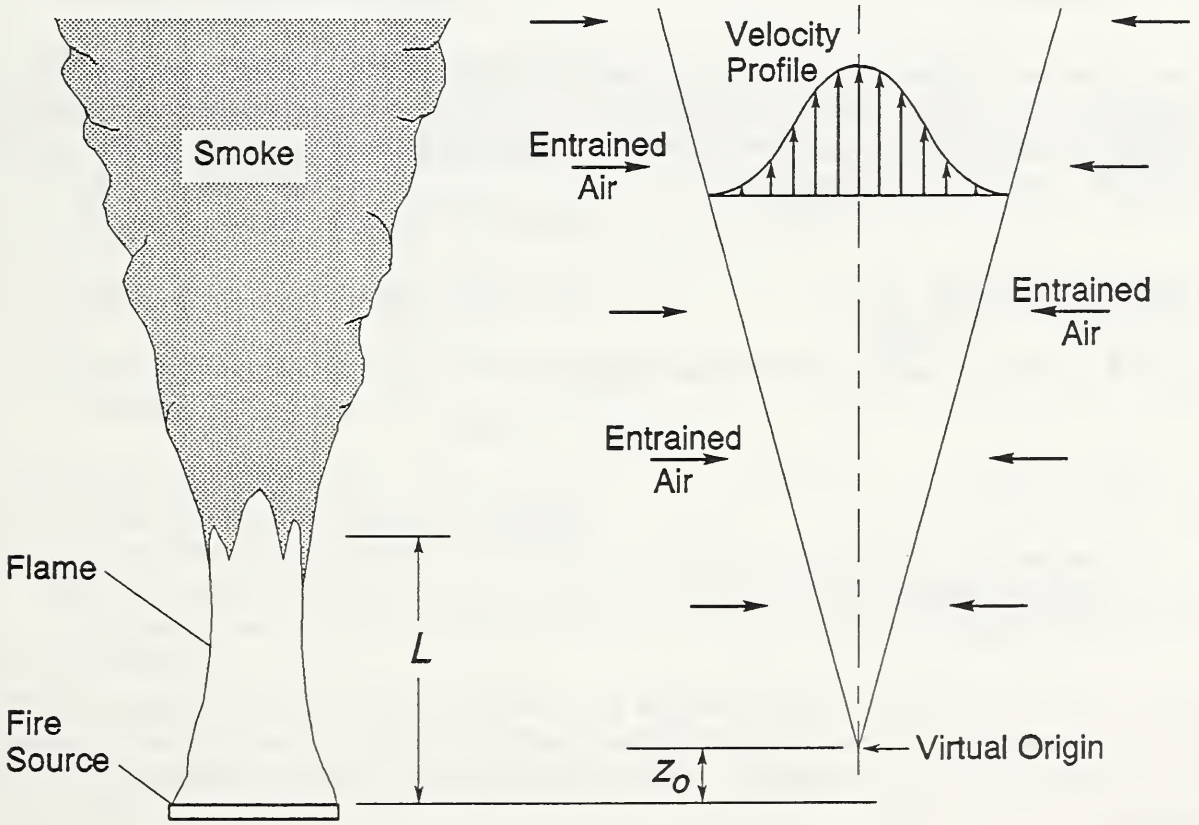

Figure 6. Fire plume and idealized model of axisymetric, point source plume

The plume of figure 6 is called an axisymmetric plume, and researchers have extended the work of Morton, Taylor and Turner to develop models of the turbulent plumes due to fires in building spaces (for example McCaffrey 1983; Cetegan, Zukoski and Kubota 1982; Heskestad 1984). Because Heskestad's plume equation and his related work were the basis of NFPA 92B (1991), these equations are used in this paper. These equations are for steady plumes, and some considerations of steady plume are discussed in Appendix H.

4.1 Mass Flow With Virtual Origin Correction

Heskestad's (1984) equation for the mass flow of an axisymmetric plume is

$$\dot{m} = C_1 Q_c^{1/3} (z - z_o)^{5/3} \left[1 + C_2 Q_c^{2/3} (z - z_o)^{-5/3}\right] \tag{3}$$

where

$\dot{m}$ = mass flow in plume at height z, kg/s (lb/s);
Q_c = convective heat release rate of fire, kW (Btu/s);
z = height above top of fuel, m (ft);
z_o = virtual origin of the plume, m (ft);
C_1 = 0.071 (0.022);
C_2 = 0.026 (0.19).

Because smoke was defined to include the air that is entrained with the products of combustion, all of the mass flow in the plume is defined as being smoke. It follows that equation (3) can be thought of as an equation for the production of smoke from a fire. A simplified plume mass equation will be presented later, and the same comments also apply to it.

4.2 Virtual Origin

Heskestad's (1983) relationship for the virtual origin is

$$z_o = C_3 Q^{2/5} - 1.02 D_f \tag{4}$$

where

Q = heat release of the fire, kW (Btu/s);
D_f = diameter of fire, m (ft);
C_3 = 0.083 (0.278).

In figure 6 the virtual origin is shown above the top of the fuel, but it can also be below the fuel. The sign convention is: for the virtual origin above the top of the fuel z_o is positive, and for the virtual origin below the top of the fuel z_o is negative. The convective portion of the heat release rate, Q_c, can be expressed as

$$Q_c = \xi Q \tag{5}$$

where ξ is the convective fraction of heat release. The convective fraction depends on the heat conduction through the fuel and the radiative heat transfer of the flames, but a value of 0.7 is often used for ξ.

4.3 Average Plume Temperature

The average temperature of the plume can be obtained from a first law of thermodynamics analysis of the plume. Consider the plume as a steady flow process with the control volume of figure 7. Neglecting the small amount of mass added to the plume flow due to combustion, the first law for the plume is

$$Q_g + Q_t = \dot{m}(h_e - h_i + \Delta KE + \Delta PE) + W \tag{6}$$

where

Q_g = heat generated within the control volume, kW (Btu/s);
Q_t = heat transferred from surroundings into the control volume, kW (Btu/s);
$\dot{m}$ = mass flow rate, kg/s (lb/s);
h_i = enthalpy of flow entering the control volume, kW/kg (Btu/s lb);
h_e = enthalpy of flow leaving the control volume, kW/kg (Btu/s lb);
ΔKE = change in kinetic energy, kW/kg (Btu/s lb);
ΔPE = change in potential energy, kW/kg (Btu/s lb);
W = work done by system on its surroundings, kW (Btu/s).

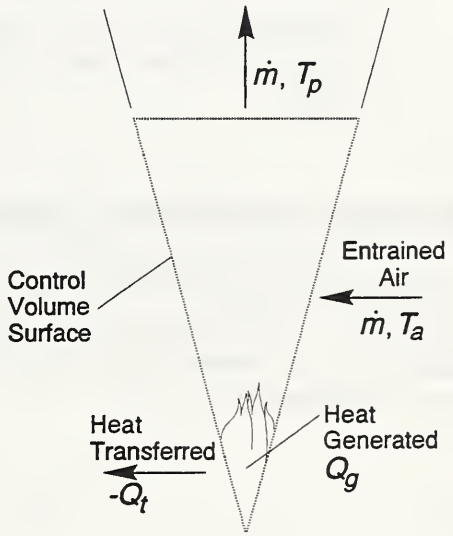

Figure 7. Control volume for idealized plume

For the steady plume the work is zero, and the changes in kinetic and potential energy are negligible. The heat generated is the heat release of the fire ($Q_g = Q$). Heat is transferred from the plume by conduction and radiation to the surroundings, so that $Q_c = Q_g + Q_t$. Specific heat can be considered constant ($h = C_p T$). The first law leads to an equation for the plume temperature:

$$T_p = T_a + \frac{Q_c}{\dot{m} C_p} \tag{7}$$

where

T_p = average plume temperature at elevation z, °C (°F);
T_a = ambient temperature, °C (°F);
C_p = specific heat of plume gases, kJ/kg °C (Btu/lb °F).

Fire plumes consist primarily of air mixed with the products of combustion, and the specific heat of plume gases is generally taken to be the same as air [C_p = 1.00 kJ/kg °C (0.24 Btu/lb °F)]. The plume mass flow equation (3) was developed for strongly buoyant plumes. For small temperature differences between the plume and ambient, errors due to low buoyancy could be significant. This topic needs study, and, in the absence of better data, it is recommended that the plume equations not be used when this temperature difference is small [less than 2°C (4°F)].

4.4 Volumetric Flow

The volumetric flow of a plume is

$$\dot{V} = C_4 \frac{\dot{m}}{\rho_p} \tag{8}$$

where

$\dot{m}$ = mass flow in plume at height z, kg/s (lb/s);
$\dot{V}$ = volumetric smoke flow at elevation z, m^3/s (cfm);
ρ_p = density of plume gases at elevation z, kg/m^3 (lb/ft^3);
C_4 = 1 (60).

4.5 Plume Centerline Temperature

The temperature from equation (7) is a mass flow average, and the temperature varies over the plume cross-section. The plume temperature is greatest at the centerline of the plume, and the centerline temperature is of interest when atria are tested by real fires as discussed later. The centerline temperature equation (Heskestad 1986) is

$$T_{cp} = T_a + C_5 \left(\frac{T_a}{g\, C_p^2\, \rho_a^2} \right)^{1/3} \frac{Q_c^{2/3}}{(z - z_o)^{5/3}} \tag{9}$$

where

T_{cp} = absolute centerline plume temperature at elevation z, K (°R);
T_a = absolute ambient temperature, K (°R);
ρ_a = density of ambient air, kg/m^3 (lb/ft^3);
g = acceleration of gravity, m/s^2 (ft/s^2);
C_5 = 9.1 (0.0067).

For the following conditions of 294 K (529°R), ρ_a of 1.2 kg/m^3 (0.075 lb/ft^3), g of 9.8 m/s^2 (32.2 ft/s^2), and C_p of 1.00 kJ/kg °C (0.24 Btu/lb °F); the centerline temperature equation becomes

$$T_{cp} = T_a + C_6 \frac{Q_c^{2/3}}{(z - z_o)^{5/3}} \quad (10)$$

where
T_p = centerline plume temperature at elevation z, °C (°F);
T_a = ambient temperature, °C (°F);
C_4 = 25 (338).

4.6 Air and Plume Gas Density

The density of air and plume gases is calculated from the perfect gas law:

$$\rho = \frac{p}{RT} \quad (11)$$

where
ρ = density of air or plume gases, kg/m^3 (lbm/ft^3);
p = absolute pressure, Pa (lbf/ft^2);
R = gas constant, J/kg K (ft lbf/lbm °R);
T = absolute temperature, K (°R).

The absolute pressure is often taken to be standard atmospheric pressure of 101,325 Pa (2116 lbf/ft^2), and the gas constant is generally taken to be that of air which is 287 J/kg K (53.3 ft lbf/lbm °R).

4.7 Plume Diameter

The diameter of a plume is approximately

$$D_p = \frac{z}{2} \quad (12)$$

where
D_p = diameter of visible plume, m (ft);
z = height above top of fuel, m (ft).

This equation is within 5% of a more complicated one that is in terms of the plume centerline temperature (NFPA 92B 1991; Klote and Milke 1992). Equation (12) is probably of sufficient accuracy for design applications, considering that plumes are in constant motion and measurement of diameter can only be approximate. Further, the visibility of smoke from different fuels varies considerably, and equation (12) may be thought of as a an indication of an upper value of likely plume diameter. Considering plume diameters can vary significantly from the estimates, plume diameter estimates need to applied conservatively. The author suggests considering plume diameter estimates to have an uncertainty in the range of plus 5% to minus 40%, until better data is available.

Equation (12) can be used to determine if geometry of a specific space lends itself to the smoke management approaches of the paper. The concern is that a plume will contact the walls of the space and fill the cross-section of the space with smoke. From equation (12), it can be said that the atrium smoke management concepts of this paper are not appropriate for spaces that are taller than twice their minimum width.

4.8 Flame Height

Equation (3) is applicable for elevations, z, that are above the mean flame height of the fire. The flame height depends on the fire geometry, the ambient conditions, the heat of combustion and the stoichiometric ratio. A relationship (Heskestad 1988) for flame height that can be used for many fuels is

$$z_f = C_7 Q^{2/5} - 1.02 D_f \tag{13}$$

where
z_f = mean flame height, m (ft);
C_7 = 0.235 (0.788).

The ceiling heights of atria are relatively high, and it is the nature of atria smoke management that the elevations, z, of interest are much greater than either virtual origin, z_o, or the flame height, z_f.

4.9 Simple Mass Flow and Flame Height Equations

If the virtual origin correction is negligible, equation (3) becomes

$$\dot{m} = C_1 Q_c^{1/3} z^{5/3} + C_8 Q_c \tag{14}$$

where
C_1 = 0.071 (0.022);
C_8 = 0.0018 (0.0042).

This is the *simple plume equation* presented in NFPA 92B. In addition to not needing to calculate z_o, the user of this equation does not need to know D_f. In design applications where the fuel is unknown, these advantages are significant. A corresponding approximate relationship for mean flame height is

$$z_f = C_9 Q_c^{2/5} \tag{15}$$

where
z_f = mean flame height, m (ft);
C_9 = 0.166 (0.533).

4.10 Discussion of Simple Equations

To evaluate the extent to which the simple equations from the section above are applicable, the fire diameter needs to be addressed. For fires that are not round, the effective diameter is defined as $D_f = 2(A/\pi)^{1/2}$ where A is the area of the fire. The heat release density of a fire is $q = Q/A$. Thus the effective diameter of a fire can be expressed as

$$D_f = 2\sqrt{\frac{Q}{\pi q}} \qquad (16)$$

Table 3 lists heat release densities for some warehouse materials (NFPA 92B 1991) and pool fires (Heskestad 1983). In this table q ranges from 90 kW/m^2 (8 Btu/s ft^2) to 14,000 kW/m^2 (1250 Btu/s ft^2). The low value is for a proprietary silicone transformer fluid, and the upper value is for polystyrene jars in compartmented cartons stacked 4.57 m (15 ft) high. These extreme fuel arrangements are not likely to be found in atria, and eliminating them results in a range of 400 kW/m^2 (35 Btu/s ft^2) to 10,000 kW/m^2 (900 Btu/s ft^2).

Figure 8 shows the effect of heat release density, q, on the location of the virtual origin. For 400 kW/m^2 (35 Btu/s ft^2), z_o is about -0.8 m (-2.6 ft) at Q of 2000 kW and -4.3 m (-14 ft) at Q of 25000 kW. The negative values of z_o indicated that the virtual origin is below the fire surface. For 10,000 kW/m^2 (880 Btu/s ft^2), z_o is about 1.2 m (3.9 ft) at Q of 2000 kW (1900 Btu/s) and 3 m (10 ft) at Q of 25000 kW (23,700 Btu/s).

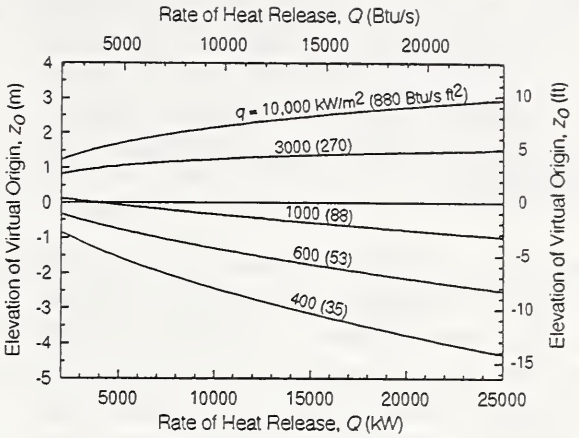

Figure 8. The effect of heat release density, q, on the elevation of the virtual origin

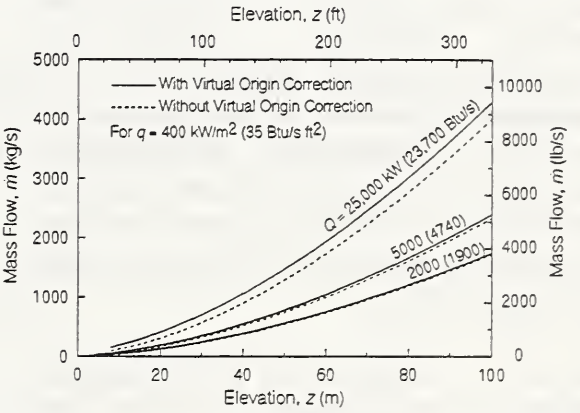
Elevation, z (ft)
With Virtual Origin Correction
Without Virtual Origin Correction
For q = 400 kW/m2 (35 Btu/s ft2)
Q = 25,000 kW (23,700 Btu/s)
5000 (4740)
2000 (1900)
Mass Flow, m (kg/s)
Mass Flow, m (lb/s)
Elevation, z (m)

Figure 9. Comparison of mass flow predictions with and without correction for virtual origin for a heat release density of 400 kW/m^2 (35 Btu/s ft^2)

Figure 9 shows the impact of the virtual origin correction on plume mass flow for q = 400 kW/m^2 (35 Btu/s ft^2), and figure 10 shows the corresponding impact for q = 10,000 kW/m^2 (880 Btu/s ft^2). Figure 9 shows that equation (14) results in under prediction for the lower heat release density, and figure 10 shows that this equation (14) results in over prediction for the higher heat release density. These over and under predictions are with reference to equation (3). Table 4 lists deviations of mass flow due to

omitting the correction. For a 20 m (67 ft) atria, these deviations range from -26% to 26%. For taller atria, the range decreases: at 40 m (130 ft) it is -15% to 13%, and at 80 m (260 ft) it is -8% to 6%. Equation (14) predicts mass flows that are about in the middle of the range of values from equation (3).

An estimate of the uncertainty of equation (3) is not available, but it should be noted that the state of plume technology is such that the above ranges may be within the uncertainty of equation (3). Further, fire spread by radiation can result in an number of nearby fires with separate plumes joining together as they rise. Theories have yet to be developed for such multiple fire plumes. There is no question that both equations (3) and (14) reflect the important trends of mass flow being a strong function of elevation, z, and a weak function of convective heat release rate, Q_c. However, to conservatively apply equation (14), it is suggested that the location of the fire surface be conservatively selected. For example, if fires may be possible anywhere from the floor level to 3 m (10 ft) above the floor, conservative selection of fire surface would be at the floor.

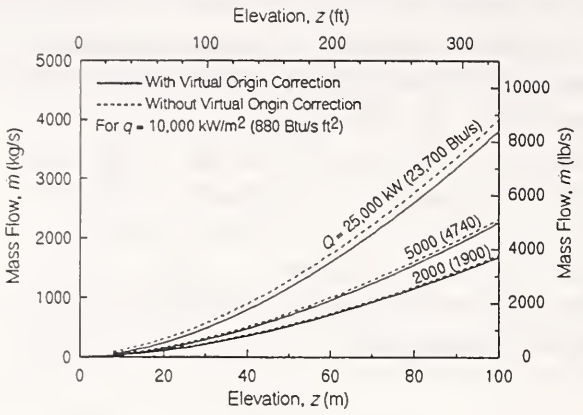

Figure 10. Comparison of mass flow predictions with and without correction for virtual origin for a heat release density of 10,000 kW/m^2 (880 Btu/s ft^2)

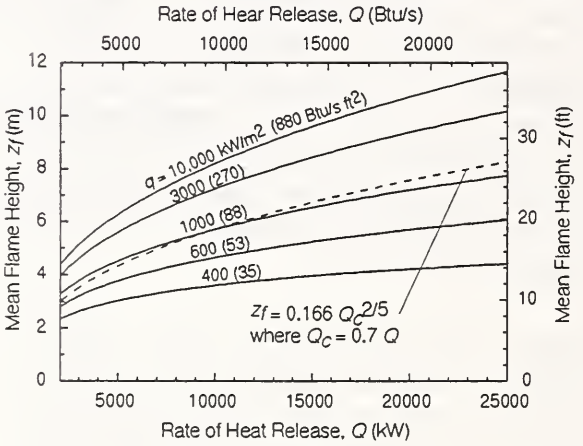

Figure 11. Comparison of predicted flame heights to the approximate equation (dashed line)

Figure 11 compares the predicted flame heights from equation (13) with the approximate relation of equation (15). Again the approximate relation is in the middle of the range of predicted values. It is apparent that flame height, z_f, increases with q. In atria smoke management design, flame height is primarily used to assure that the plume mass flow equations are appropriate. The flame height, z_f, ranges from 2.4 m (8 ft) to 4.4 m (14 ft) at 2000 kW (1900 Btu/s) and from 4.3 m (14 ft) to 12 m (39 ft)at 25000 kW (23,700 Btu/s).

To make the calculations based on the above plume equations, ASMET menu items "**Simple Plume Equations**" and "**Plume With Virtual Origin Correction**" can be used.

Table 3. Heat release density of some materials

	Material Burned	Heat Release Density, q kW/m^2	Btu/s ft^2
1.	Wood pallets, stacked 0.46 m (1.5 ft) high (6-12% moisture)	1400	125
2.	Wood pallets, stacked 1.52 m (5 ft) high (6-12% moisture)	4,000	350
3.	Wood pallets, stacked 3.05 m (10 ft) high (6-12% moisture)	6,800	600
4.	Wood pallets, stacked 4.88 m (16 ft) high (6-12% moisture)	10,000	900
5.	Mail bags, filled, stored 1.52 m (5 ft) high	400	35
6.	Cartons, compartmented, stacked 4.57 m (15 ft) high	1,700	150
7.	PE letter trays, filled, stacked 1.52 m (5 ft) high on cart	8,500	750
8.	PE trash barrels in cartons, stacked 4.57 m (15 ft) high	2,000	175
9.	PE fiberglass shower stalls in cartons, stacked 4.57 m (15 ft) high	1,400	125
10.	PE bottles packed in item 6	6,200	550
11.	PE bottles in cartons, stacked 4.57 m (15 ft) high	2,000	175
12.	PU insulation board, rigid foam, stacked 4.57 m (15 ft) high	1,900	170
13.	PS jars packed in item 6	14,000	1,250
14.	PS tubes nested in cartons, stacked 4.27 m (14 ft) high	5,400	475
15.	PS toy parts in cartons, stacked 4.57 m (15 ft) high	2,000	180
16.	PS insulation board, rigid foam, stacked 4.27 m (14 ft) high	3,300	290
17.	PVC bottles packed in item 6	3,400	300
18.	PP tubes packed in item 6	4,400	390
19.	PP & PE film in rolls, stacked 4.27 m (14 ft) high	6,200	550
20.	Methanol pool, 0.16 m (0.52 ft) diameter	2,000	180
21.	Methanol pool, 1.22 m (4.0 ft) diameter	400	35
22.	Methanol pool, 1.74 m (5.7 ft) diameter	400	35
23.	Methanol pool, 2.44 m (8.0 ft) diameter	420	37
24.	Methanol pool, 0.97 m (3.2 ft) square	745	66

Table 3. Continued Heat release density of some materials

	Material Burned	Heat Release Density, q kW/m^2	Btu/s ft^2
25.	Silicone transformer fluid pool, 1.74 m (5.7 ft) diameter	90	8
26.	Silicone transformer fluid pool, 2.44 m (8.0 ft) diameter	90	8
27.	Hydrocarbon transformer fluid pool, 1.22 m (4.0 ft) diameter	940	83
28.	Hydrocarbon transformer fluid pool, 1.74 m (5.7 ft) diameter	900	80
29.	Heptane pool, 1.22 (4 ft) diameter	3,000	270
30.	Heptane pool, 1.74 (5.7 ft) diameter	3,200	280

Notes:
1. Abbreviations are: PE = polyethylene, PS = polystyrene, PVC = polyvinyl chloride, PP = polypropylene, PU = polyurethane.
2. Items 1 through 19 from NFPA 92B (1991).
3. Items 20 through 30 from Heskestad (1983).
4. Items 25 through 28 are proprietary products.

Table 4. Deviations of mass flow due to omitting the virtual origin correction

Heat Release Rate, Q		Heat Release Density, q		Elevation above the fire, z		
kW	Btu/s	kW/m^2	Btu/s ft^2	20 m (67 ft)	40 m (130 ft)	80 m (260 ft)
2,000	1,900	400	35	-7%	-3%	-2%
5,000	4,740	400	35	-11%	-6%	-3%
25,000	23,700	400	35	-26%	-15%	-8%
2,000	1,900	10,000	880	10%	5%	3%
5,000	4,740	10,000	880	15%	7%	4%
25,000	23,700	10,000	880	26%	13%	6%

5. Approaches for Smoke Management

Most atria smoke management systems are designed with the goal of not exposing occupants to smoke during evacuation[1]. The following are approaches that can be used to manage smoke in atria:

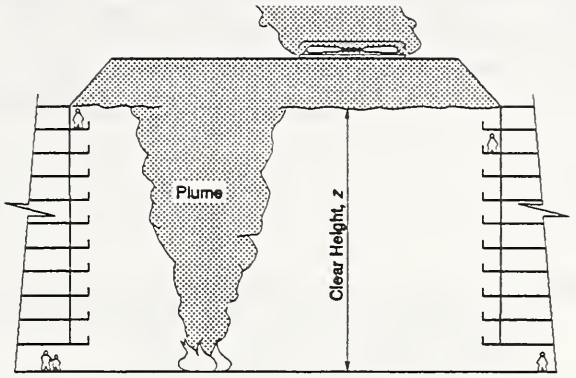

Figure 12. Smoke exhaust to maintain constant clear height

1. **Filling With a Steady Fire**: This approach consists of allowing smoke to fill the atria space while occupants evacuate the atria. This approach applies only to large volume spaces where the smoke filling time is sufficient for both decision making and evacuation. For information about people movement during evacuation, the reader is referred to Nelson and MacLennan (1988) and Pauls (1988). The smoke filling calculations are based on a steady design fire, and these calculations can be done by the computer zone fire models discussed above or by application of the *steady filling equation* presented in the next section.

2. **Filling with an Unsteady Fire**: The comments for approach 1 apply except that the fire is unsteady. Smoke filling calculations by a t-squared fire can be done by the *unsteady filling equation* presented later. As with approach 1, the smoke filling calculations can also be done by computer zone fire models. The computer approach allows simulation of filling by other than t-squared fires, including those illustrated in figure 3.

3. **Steady Clear Height With Upper Layer Exhaust**: This approach consists of exhausting smoke from the top of the atrium in order to achieve a steady clear height for a steady fire (figure 12). A calculation method based on the plume equations above is presented later. Computer zone fire models can also be used for these calculations.

4. **Unsteady Clear Height With Upper Layer Exhaust**: This approach consists of exhausting smoke from the atrium top at a rate such that occupants will have sufficient time for decision making and evacuation. The most convenient analysis method for this design approach is by a computer zone fire model, and is not discussed further in this paper.

---

[1]An alternate goal is not to subject occupants to untenable conditions. Possibly the reason that this approach is not commonly accepted is the reluctance of engineers to design systems that expose occupants to any smoke even if that exposure is not lethal.

5.1 Filling by a Steady Fire

The following experimental correlation of the accumulation of smoke in a space due to a steady fire is the *steady filling* equation from NFPA 92B:

$$\frac{z}{H} = C_{10} - 0.28 \ln\left(\frac{t Q^{1/3} H^{-4/3}}{\frac{A}{H^2}}\right) \tag{17}$$

where

z = height of the first indication of smoke above the fire, m (ft);
H = ceiling height above the fire, m (ft);
t = time, s;
Q = heat release rate from steady fire, kW (Btu/s);
A = cross-sectional area of the atrium, m^2 (ft^2);
C_{10} = 1.11 (0.67).

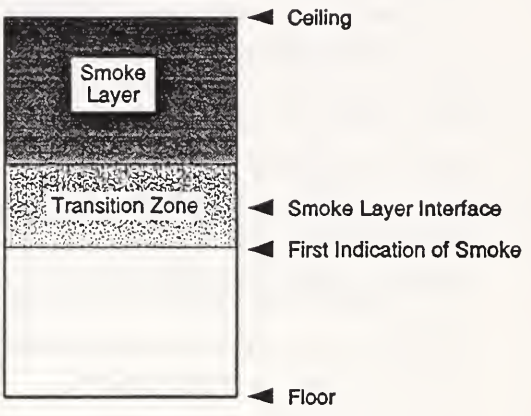

Figure 13. Smoke layer interface

This equation is conservative in that it estimates the height of the first indication of smoke above the fire rather than the smoke interface as illustrated in figure 13. In the idealized zone model, the smoke interface is considered to be a height where there is smoke above and none below. In actual fires there is a gradual transition zone between the lower cool layer and upper hot layer. The first indication of smoke can be thought of as the bottom of the transition zone. Equation (17) is based on a plume that has no contact with the walls. Because wall contact reduces entrainment of air, this condition is conservative.

Equation (17) is for a constant cross-sectional area with respect to height. For other atrium shapes physical modeling or CFD can be used. Alternatively, a sensitivity analysis can be made using the above equation to set bounds on the filling time for an atrium of complex shape. The equation is appropriate for A/H^2 from 0.9 to 14 and for values of z greater than or equal to 20% of H. A value of z/H greater than one means that the smoke layer under the ceiling has not yet begun to descend. These conditions can be expressed as

$$A = \text{Constant with respect to } H,$$

$$0.2 \le \frac{z}{H} < 1.0 \quad ,$$

and

$$0.9 \le \frac{A}{H^2} \le 14 \quad .$$

When equation (17) is solved for z/H, the user will find that z/H is often outside the acceptable range. The steady filling equation can be solved for time.

$$t = \frac{A}{H^2}\frac{H^{4/3}}{Q^{1/3}}\exp\left[\frac{1}{0.28}\left(C_{10} - \frac{z}{H}\right)\right] \tag{18}$$

To make the calculations based on the equations of this section, ASMET menu items "**Steady Filling Equation (Solve for z)**" and "**Steady Filling Equation (Solve for t)**" can be used.

5.2 Filling by an Unsteady Fire

For a t-squared fire, the location of the smoke layer interface can be estimated by the *unsteady filling equation* from NFPA 92B:

$$\frac{z}{H} = C_{11}\left[t\, t_g^{-2/5} H^{-4/5}\left(\frac{A}{H^2}\right)^{-3/5}\right]^{-1.45} \tag{19}$$

where
z = height of the first indication of smoke above the fire, m (ft);
H = ceiling height above the fire, ft (m);
t = time, s;
t_g = growth time, s;
A = cross-sectional area of the atrium, m^2 (ft^2);
C_{11} = 0.91 (0.23).

This equation is also based on experimental data and is conservative in that it estimates the height of the first indication of smoke and is for a plume that has no wall contact.

Equation (19) is also for a constant cross-sectional area with respect to height, and the comments about atria of other shapes in the section above also apply to this section. The equation is appropriate for A/H^2 from 1.0 to 23 and for values of z greater than or equal to 20% of H. A value of z/H greater than one also mean that the smoke layer under the ceiling has not yet begun to descend. These conditions can be expressed as

$$A = \text{Constant with respect to } H,$$

$$0.2 \le \frac{z}{H} < 1.0 \quad ,$$

and

$$1 \le \frac{A}{H^2} \le 23 \quad .$$

The growth time, t_g, has already been discussed, and values of it for various characteristic fire growths are listed in table 2. As with the steady filling equation, the unsteady filling equation can be solved for time:

$$t = C_{12} t_g^{2/5} H^{4/5} \left(\frac{A}{H^2}\right)^{3/5} \left(\frac{z}{H}\right)^{-0.69} \quad (20)$$

where C_{12} is 0.937 (0.363).

To make the calculations based on the equations of this section, ASMET menu items **"Unsteady Filling Equation (Solve for z)"** and **"Unsteady Filling Equation (Solve for t)"** can be used.

5.3 Steady Clear Height With Upper Layer Exhaust

The method of analysis presented in this section is based on several simplifying assumptions, and before using this method designers must verify that these assumptions are appropriate for their application.

As already stated, figure 12 illustrates smoke exhaust from an atrium to maintain a steady clear height. A consequence of the steady clear height consideration is that the design fire must be of constant heat release rate. Consider that the only flow into the smoke layer is from the plume, and the only flow from the smoke layer is the smoke exhaust. From the principle of conservation of mass for a steady process, the exhaust flow must equal the flow from the plume. Equation (14) can be used to calculate the exhaust flow rate, and this equation is listed below with variables redefined for this application:

$$\dot{m} = C_1 Q_c^{1/3} z^{5/3} + C_8 Q_c \quad (21)$$

where

$\dot{m}$ = mass flow exhaust of exhaust air, kg/s (lb/s);
Q_c = convective heat release rate of fire, kW (Btu/s);
z = clear height above top of fuel, m (ft);
C_1 = 0.071 (0.022);
C_8 = 0.0018 (0.0042).

The clear height is from the top of the fuel to the interface between the "clear" space and the smoke layer. As already stated, it is suggested that the top of the fuel be considered at the floor level to compensate for the uncertainties of the plume equation (figure 12).

For an upper layer with little heat transfer to the atrium walls and ceiling and small radiative losses from the smoke layer, the upper layer can be thought of as being *adiabatic* or as having negligible heat transfer. Based on equation (6), the adiabatic exhaust temperature is

$$T_p = T_a + \frac{Q_c}{\dot{m} C_p} \quad (22)$$

where

T_p = adiabatic exhaust temperature, °C (°F);
T_a = ambient temperature, °C (°F);

$\dot{m}$ = mass flow of exhaust air, kg/s (lb/s);
Q_c = convective heat release rate of fire, kW (Btu/s);
C_p = specific heat of plume gases, kJ/kg °C (Btu/lb °F).

The density of the exhaust gases can be calculated from the perfect gas law:

$$\rho = \frac{p}{RT} \tag{23}$$

where
ρ = density of exhaust gases, kg/m^3 (lbm/ft^3);
p = absolute pressure, Pa (lbf/ft^2);
R = gas constant, J/kg K (ft lbf/lbm °R);
T = absolute temperature of exhaust gases, K (°R).

The volumetric flow of exhaust gases in plume is

$$\dot{V} = C_4 \frac{\dot{m}}{\rho_p} \tag{24}$$

where
$\dot{m}$ = mass flow of exhaust air, kg/s (lb/s);
$\dot{V}$ = volumetric flow of exhaust gases, m^3/s (cfm);
ρ_p = density of exhaust gases, kg/m^3 (lb/ft^3);
C_4 = 1 (60).

The major assumptions of the above analysis are listed below.

1. The simple plume mass flow equation is appropriate for atria smoke management applications.
2. The heat release rate of the fire is constant.
3. The clear height is greater than the mean flame height.
4. The smoke layer is adiabatic.
5. The plume flow and the exhaust are the only significant mass flows into or out of the smoke layer.

The applicability of simple plume equations have been discussed above, and it was concluded that they are appropriate for atrium design applications. The appropriateness of assumption 2 can be checked by equation (15) or figure 11. Generally smoke layers in atria are not adiabatic, but the adiabatic assumption is both useful and conservative. Without this assumption, the analysis would be complicated by the incorporation of heat transfer. The assumption is conservative in that incorporating heat transfer results in lower volumetric flow rates of exhaust air. Thus assumption 3 may not be true, but it is conservative and results in a simplified analysis. With regard to assumption 4, the potential for leakage from the outside or from other building spaces to the smoke layer should be checked. If such flows exist the analysis can be modified by increasing the exhaust flow accordingly.

If the smoke layer is not deep enough relative to the exhaust inlets, there is the possibility of pulling some air from below the smoke layer into the exhaust, and this would reduce the effectiveness of the exhaust

system. Such reduced effectiveness would result in a smoke layer interface going below the design value and could expose occupants to smoke. Currently, designers use engineering judgement in the selection of this height, however ASHRAE's Fire and Smoke Control Committee is developing a research project to study this issue.

To make the calculations based on the equations of this section, ASMET menu item "**Simple Plume Equations**" can be used. The variables of this menu are identified by the plume flow terminology so that the user will be reminded of the basis of these equations.

6. Pre-Stratification and Detection

Often a hot layer of air forms under the ceiling of an atrium, the result of solar radiation on the atrium roof. While studies have not been made of this *pre-stratification* layer, building designers indicate that the temperatures of such layers are often in excess of 50°C (120 °F). Temperatures below this layer are controlled by the building's heating and cooling system, and temperature profile can be considered to increase significantly over a small increase in elevation as shown in figure 14. An analysis of smoke stratification is given in NFPA 92B, but it is not appropriate for the temperature profile addressed of this section[2].

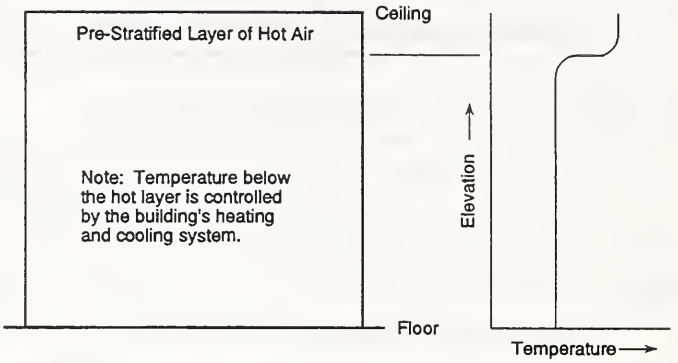
Ceiling
Pre-Stratified Layer of Hot Air
Note: Temperature below the hot layer is controlled by the building's heating and cooling system.
Elevation
Floor
Temperature

Figure 14. Pre-stratified layer of hot air under atrium ceiling and the resulting temperature profile

When the average temperature of the plume is less than that of the pre-stratification layer, the smoke will form a stratified layer under it as shown in figure 15. Average plume temperatures can be calculated from equations (6) and (14), and they are graphed in figure 16. It can be observed from figure 16 that the average plume temperature is usually less than expected temperatures of the hot air layer. Thus when there is a hot pre-stratified air layer, smoke cannot be expected to reach the ceiling of the atrium, and smoke detectors mounted on that ceiling cannot be expected to go into alarm.

Beam smoke detectors used to detect smoke in the plume can overcome the limitations of ceiling mounted detectors in atria. Generally the light beams are oriented horizontally. Beam detectors are often mounted on balconies, where they are generally easier to reach for maintenance than are detectors that are mounted on the ceilings of the atrium. The beams need to be below the pre-stratified hot layer, and the space

---

[2]The analysis of smoke stratification in NFPA 92B is for a constant temperature increase per unit elevation (dT/dz = constant). This analysis does not apply to the pre-stratification layer that forms under the atrium ceiling. When conditions of constant dT/dz exist in a large space, the NFPA 92B approach can be used to estimate the maximum height of smoke rise.

between beams needs to be small enough so that plumes will be detected regardless of where the fire is located. As already stated, equation (12) describes the visible plume diameter with an estimated uncertainty in the range of plus 5% to minus 40%. Therefore, it is suggested that the spacing between beams be:

$$x = \frac{H_b}{4} \qquad (25)$$

where

x = minimum spacing between light beams, m (ft);

H_b = height of beams above floor, m (ft).

The height of beams above the floor, H_b, needs to be well below the pre-stratification layer so that the plume will reach the level of the beams and be detected. Figure 17 is an example arrangement of beam detectors in an atrium.

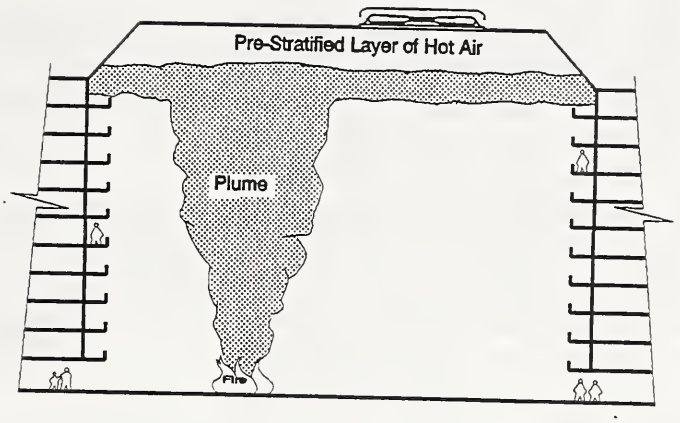

Figure 15. Smoke filling a pre-stratified atrium

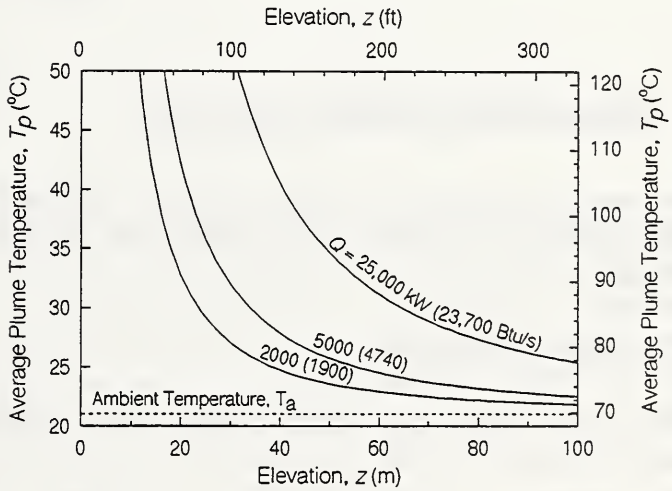

Figure 16. Average plume temperature calculated from equations (6) and (14)

7. Make-Up Air

The same mass flow rate of air exhausted from the top of the atrium needs to enter the atrium below the smoke layer. One approach is to introduce this air through openings to the outside such as open doors and louvers that automatically open upon system activation. Where such openings are not practical, make-up air can be supplied by a fan powered system. The velocity of makeup air should not deflect the plume significantly which would increase entrainment. At locations where the makeup airflow could contact the plume, the velocity of this airflow should not exceed about 1 m/s (200 fpm).

8. Separated Spaces

Spaces away from the atrium can either be separated from the atrium or they can be open to the atrium. *Separated spaces* are isolated from the atrium by smoke barriers, and these smoke barriers are either

vertical or horizontal membranes that are designed and constructed to resist the movement of smoke. Walls, floors and ceilings can be smoke barriers, and these barriers may have a fire resistive rating. Smoke barriers may have doorways or other openings that are protected by automatically closing devices such as doors or dampers. Separated spaces can rely on the integrity of the smoke barriers or can also rely on smoke control by pressurization as addressed in NFPA 92A (1993) and Klote and Milke (1992).

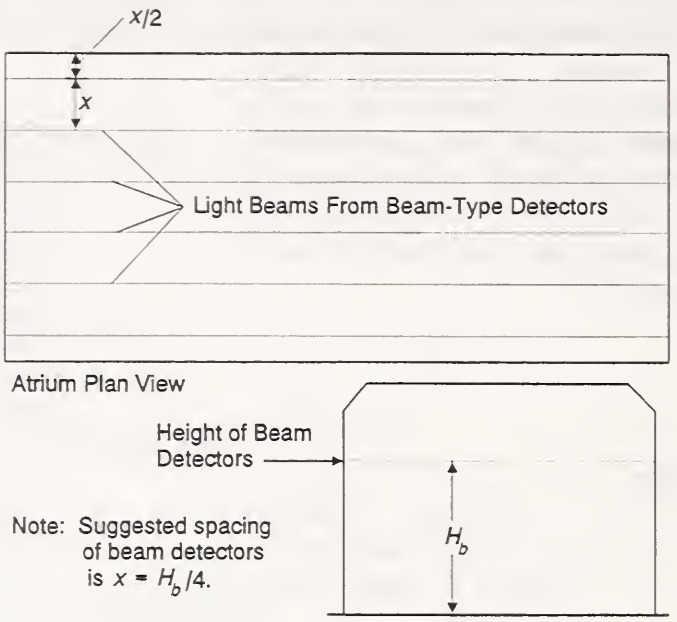

Figure 17. Beam detectors used for activation of atrium smoke management system

9. Communicating Spaces

Communicating spaces are spaces within a building that have an open pathway to an atrium. The communicating spaces may open directly into the atrium or they may be connected through an open passage.

9.1 Other Plumes

Balcony spill plumes and window plumes are both addressed in NFPA 92B and by Klote and Milke as means of smoke flow into the atrium from a fire in a communication space. The method of analysis of these plumes is based on there being hot, buoyant smoke flowing into the atrium. If the fires in the communicating spaces are sprinklered, the resulting smoke is neither hot nor buoyant. Considering that the communicating spaces in most new buildings with atria in the United States are sprinklered, this paper does not address spill plumes or window plumes.

It may be possible to have an atrium building (possibly retrofit) without sprinklers in communicating spaces, and these other plumes should be considered in the analysis of an atrium system.

9.2 Airflow for a Communicating Space Fire

Airflow can be used to prevent smoke from flowing from a fire in a communicating space to the atrium. The intent of this approach is to protect the atrium and non-fire communicating spaces. The fundamental question concerning this approach is what level of protection is provided. Currently, there is insufficient

information to evaluate whether these systems provide any significant level of protection to life or if their sole benefit is property protection[3].

The issue of evaluation of the potential benefit of this approach is further complicated by the concern about airflow supplying combustion air for a fire. Klote and Milke (1992) address this issue, and they recommend that airflow not be used for smoke control, except when the fire is suppressed or in the rare cases when fuel can be restricted with confidence.

If it is desired to use airflow to prevent smoke originating in the communicating space from flowing into the atrium, the air needs to be exhausted from the communicating space. The exhaust flow rate needs to be sufficient to result in an average air velocity in the opening between the communicating space and the atrium to prevent smoke flow. NFPA 92B recommends the following equation by Heskestad (1989) for the limiting velocity to prevent smoke backflow:

$$V = C_{13}\sqrt{\frac{gH(T_f - T_o)}{T_f}} \tag{26}$$

where
V = average air velocity, m/s (ft/min);
g = acceleration of gravity, m/s^2 (ft/s^2);
H = height of opening, m (ft);
T_f = temperature of heated smoke, K (°R);
T_o = temperature of ambient air, K (°R);
C_{13} = 0.64 (38).

Determination of realistic temperatures of smoke from a sprinklered fire is difficult. Lui (1977) studied the evaporative cooling of sprinkler spray on fire gases and showed that smoke temperatures were sometimes cooled below ambient temperature. NFPA 92B indicates that 74°C (165°F) is considered realistic for sprinklered fires. In the absence of good data applicable to the above equation, the indicated temperature was the best advice that the committee was able to give on this subject. Before sprinklers take effect, the elevated gas temperature is restricted to in a thin layer [0.05 to 0.1 m (2 to 4 in)] below the ceiling. After sprinklers activated, this temperature may be conservatively high, considering the findings of Lui.

Research is needed to evaluate the potential benefits of these airflow systems. If the benefits support use of these systems, research is needed to develop an approach that can be applied to sprinklered fires with more confidence than the approach above.

---

[3]Based on fires evaluated by Madrzykowski (1991), it would seem that sprinklered fires of office building materials in typical configurations would not result in lethal conditions in spaces away from the room of fire origin even for fires that are shielded from the sprinkler spray. However, Mawhinney and Tamura (1994) conducted a series of very well shielded and massive wood fires that resulted in the production of significant levels of carbon monoxide. Because there is a question as to the applicability of Mawhinney and Tamura's wood fires to commercial buildings, Mawhinney is conducting a study to evaluate this issue.

9.3 Airflow for an Atrium Fire

Airflow can also be used to prevent smoke from flowing from the atrium to the communicating space. The comments from the section above about the uncertainty of the level of protection provided also apply to the systems of this section.

Air can be supplied to a communicating space to achieve a specific average velocity at the opening to the atrium. This velocity should be such that smoke flow to the communicating space is prevented. For opening locations below the smoke layer and 3 m (10 ft) above the base of the fire, the NFPA 92B equation for this velocity is

$$V = C_{14}\left(\frac{Q}{z}\right)^{1/3} \tag{27}$$

where
V = average air velocity, m/s (ft/min);
Q = heat release rate of the fire, kW (Btu/s);
z = distance above the base of the fire to the bottom of the opening, m (ft);
C_{14} = 0.057 (17).

If the velocity calculated from the above equation is greater than 1 m/s (200 fpm), then a velocity of 1 m/s (200 fpm) should be used. This limitation was made out of concern that greater velocities could disrupt the plume flow and have an adverse effect on atrium smoke management.

For openings above the smoke layer interface, equation (26) should be used to calculate the velocity. The above equation was provided for NFPA 92B by Heskestad and is based on unpublished theoretical considerations. As with the section above, research is needed concerning airflow and fires in the atrium.

10. Commissioning and Acceptance Testing

Commissioning is needed to assure that smoke control systems will function as intended during fire situations. Many designers and builders have told this author that they believe that acceptance testing is the major problem with smoke control systems. They say that everything goes well up to testing, and then the system fails to pass the tests required by the local authority. However, acceptance testing is not the major problem, it is the symptom of the real problems. A commissioning approach can reduce the potential for difficulties during the acceptance test. The guideline for commissioning (ASHRAE 5, 1994) includes the following:

1. Pre-Design Phase,
2. Design Phase,
3. Construction Phase,
4. Acceptance Procedures, and
5. Post-Acceptance Phase.

The pre-design phase includes identification of objectives and initial development of a commissioning plan. The design phase includes documentation of design criteria, assumptions, description of system, description of required performance, test procedure, project schedule, and system certification. The basic principle behind selection of a test procedure is that the test needs to verify system performance under fire conditions. Construction phase includes review of submittals for equipment and controls, as well as, testing, adjusting and balancing of air moving systems. Acceptance procedures includes preparation for the test, conducting the test, and documentation of the test results. Post-acceptance efforts include maintenance, any system modifications, and documentation.

10.1 Fire Tests

A real fire is the most realistic method of testing a smoke control system. It is an understatement to say that the construction community has concerns about the danger of building fires in atria. The information in this brief section is intended to give the reader an idea of what can be done concerning real fire tests, and readers wishing to conduct such tests should start by making an exhaustive investigation into the topic.

Real fire tests of atria smoke management systems are common in Australia (Atkinson 1992; Atkinson and Marchant 1992), and one such test has been conducted in the United States (Dillon 1994). The Australian tests use ethyl alcohol pool fires of 1000 to 5000 kW, and chemical smoke tracer[4] to make the plume and smoke layer visible. Dillon used a propane fire of 5000 kW with a different chemical smoke tracer[5]. While the propane fire was more expensive, it had the safety advantage that it could shut off quickly by closing a valve. Determination of the heat release rate is probably more accurate with the propane by metering the flow and having propane of certified heating value.

Because of concern about heat damage to ceiling and structural members, the centerline plume temperature should be calculated before the test. Atkinson and Marchant indicate that these estimates have been wrong on a few occasions, and they provide an alternative mass weighted calculation that requires iteration. They also indicate that these real fire tests require attention to detail, and they express concern about the danger that could result from badly applied tests.

10.2 Performance Tests Without a Fire

Performance tests without a fire consist of measuring the performance of the system components to assure that these are functioning as intended during system design. For an atrium exhaust system, this would consist of measuring the exhaust flow and any other flows that are part of the design. For a system that has been designed by a professional engineer upon accepted engineering principles (like those discussed in this paper), these flow measurements are a sufficient indication that the system will perform as desired under fire conditions.

---

[4]The tracer was Nico which is a brand name, but mention of this product is neither a recommendation nor an endorsement of the product.

[5]The tracer was Military HC which is a brand name, but mention of this product is neither a recommendation nor an endorsement of the product.

10.3 Chemical Smoke Tracer Tests

Chemical smoke from smoke bombs or smoke generators can be used to test for smoke feedback into supply air. The general procedure for testing with chemical smoke is described here. A number of smoke bombs are placed in a metal container, and all bombs are simultaneously ignited. The container is located near an exhaust inlet in the smoke zone being tested so that all of the chemical smoke produced by the bombs is drawn directly into the exhaust air stream. If chemical smoke is detected in the supply air, its path should be determined, the path should be blocked, and then the smoke feedback test should be conducted again.

For pressurization systems located in spaces separated from the atrium, chemical smoke or other tracers can be useful in locating the leakage paths that sometimes defeat a smoke control system. For example, if the construction of a stairwell is unusually leaky, pressurization of that stairwell may not be possible with fans sized for construction of average tightness. Chemical smoke generated within the stairwell will flow through the leakage paths and indicate their location so that they can be caulked or sealed.

10.4 Caution About Chemical Smoke

A caution needs to be given concerning the use of chemical smoke. In the absence of a real fire, this chemical smoke has little or no buoyancy. Chemical smoke does not move like hot smoke from a flaming fire. The unrealistic nature of smoke tests from smoke bombs was illustrated by the experiments at the Plaza Hotel (Klote 1990).

Because chemical smoke tests do not test the system with a realistic fire plume, the test results cannot determine system performance against real fire conditions. It is possible that a system that would fail a chemical smoke test could perform as intended during a fire. Conversely, a system that passed a chemical smoke test could fail to perform during a fire. A serious concern with smoke bomb tests is that they can give building occupants and fire service officials a false sense of the security.

11. Summary and Conclusions

1. The approach of atrium exhausting presented in this paper and in NFPA 92B is based on the fundamentals of plume mechanics, and designers can have a level of confidence in systems designed to these principles. As with all systems, designers need to exercise care that they are within the limitations of the technology and design fires must be large enough realistically to reflect the high probability of transient fuels.

2. Exhaust is not necessary for an atrium of sufficient filling capacity such that occupants have time for both decision making and evacuation before the smoke fills to where they are located. Approaches to atrium filling (sections 5.1 and 5.2) can be used to obtain a conservative estimate of filling time. These calculations can be done by computer zone fire models

3. For situations where basic methods of 1 and 2 above are not applicable, physical modeling and CFD analysis can be used for design. The basic approaches are not applicable when the design

exceeds the range of applicability of the equations or when obstructions in an atrium do not allow plume flow.

4. Often a hot layer of air forms under the ceiling of an atrium, and this hot layer can prevent smoke from reaching the ceiling. Therefore, ceiling mounted smoke detectors are generally not recommended for atrium applications. Beam smoke detectors used to detect smoke in the plume as described in the text are recommended.

5. Commissioning is needed to assure that smoke control systems will function as intended during fire situations. Commissioning efforts should start before design and extend to maintenance system modifications after construction is finished.

6. There is concern about exhaust effectiveness for relatively thin smoke layers. There is the possibility of pulling some air from below the smoke layer into the exhaust, and this could expose occupants to smoke. Such reduced effectiveness would result in a smoke layer interface going below the design value and could expose occupants to smoke. Research is needed concerning the depth of smoke layer required to prevent atrium exhaust from pulling air from the lower layer.

7. Research is needed concerning use of airflow for smoke control between the atrium and communicating spaces. Information is needed to evaluate the potential benefits of these airflow systems. If the benefits support use of these systems, research is needed to develop new approaches for sprinklered fires.

12. Acknowledgements

The author wishes to recognize the effort of Charles Arnold for writing the computer code of ASMET. Thanks are due to Jim Quintiere and Gunnar Heskestad. Jim Quintiere was my supervisor for several years at NIST, and I have worked with Gunnar Heskestad on NFPA 92B. Both have given freely of their knowledge, and I thank them. Credit is also due to my current management, Dick Bukowski, Dave Evans, and Jack Snell for supporting this effort. Appreciation is expressed to William (Doug) Walton for support concerning the adaptation of his ASET-B model including the documentation.

13. Nomenclature

a = fire growth coefficient
A = cross-sectional area of the atrium
C = constant
C_p = specific heat of plume gases
D_f = diameter of fire
D_p = diameter of visible plume
g = acceleration of gravity
H = height of opening or of ceiling above the floor
H_b = height of beams above floor
h_e = enthalpy of flow leaving the control volume
h_i = enthalpy of flow entering the control volume
$\dot{m}$ = mass flow rate
p = absolute pressure
Q = heat release rate
Q_c = convective heat release rate
Q_g = heat generated within the control volume
Q_t = heat transferred from surroundings into the control volume
R = gas constant
t = time
T = temperature
T_a = ambient temperature
T_{cp} = centerline plume temperature
T_f = temperature of heated smoke
t_g = growth time
t_o = effective ignition time
T_o = temperature of ambient air
T_p = adiabatic exhaust temperature or average plume temperature at elevation z
V = average air velocity
$\dot{V}$ = volumetric smoke flow at elevation
W = work done by system on its surroundings
x = minimum spacing between light beams
z = clear height above top of fuel or height of the first indication of smoke above the fire
z_f = mean flame height
z_o = virtual origin of the plume
ΔKE = change in kinetic energy
ΔPE = change in potential energy
ξ = convective fraction of heat release
ρ = density
ρ_a = density of ambient air
ρ_p = density of plume gases at elevation z or density of exhaust gases

14. References

ASHRAE 5, 1994. Guideline - Commissioning Smoke Management Systems, American Society of Heating and Air-Conditioning Engineers, Atlanta, GA.

Atkinson, B. 1992. Fire Safety Engineering: The Development of an Australian Standard Hot Smoke Test for Large Compartments, 2nd CIB Workshop at the Fire Research Station, Jan 30-31, 1992, Borehamwood, UK.

Atkinson, B. and Marchant, R. 1992. Case Study The Deeds Road Experiments, Proceedings of the International Fire Safety Engineering Conference, 18-20 October 1992, Sydney Australia.

BOCA 1993. National Building Code, 12th ed, Building Officials & Code Administrators International, Country Club Hills, IL.

Bukowski, R.W. 1991. Fire Models, the Future is Now!, NFPA Journal, No 85, Vol 2, pp 60-69, March/April.

Bukowski, R.W., Peacock, R.D., Jones, W.W. and Forney, C.L. 1991. Technical Reference Guide for HAZARD I Fire Hazard Assessment Method, Version 1.1, NIST Handbook 146, Vol II, National Institute of Standards and Technology, Gaithersburg, MD.

Cetegan, B.M., Zukoski, E.E. and Kubota, T. 1982. Entrainment and Flame Geometry of Fire Plumes, PhD. Thesis of Cetegen, California Institute of Technology, Pasadena.

Cooper, L.Y. 1985. ASET - A Computer Program for Calculating Available Safe Egress Time, Fire Safety Journal, Vol 9, pp 29-45.

Cooper, L.Y. and Forney, G.P. 1987. Fire in a Room with a Hole: A Prototype Application of the Consolidated Compartment Fire Model (CCFM) Computer Code, Presented at the 1987 Combined Meetings of Eastern Section of Combustion Institute and NBS Annual Conference on Fire Research.

Degenkolb, J.G. 1975. Firesafety for Atrium Type Buildings, Building Standards, Vol 44, No 2, pp 16-18.

Degenkolb, J.G. 1983. Atriums, Building Standards, Vol 52, No 1, pp 7-14.

Dillon, M.E. 1994. Case Study of Smoke Control System Testing for a Large Enclosed Stadium, ASHRAE Transactions, Vol 100, Part 2.

Fang, J.B. and Breeze, J.N. 1980. Fire Development in Residential Basement Rooms, National Bureau of Standards, NBSIR 80-2120.

Hansel, G.O. and Morgan, H.P. 1994. Design Approaches for Smoke Control in Atrium Buildings, Fire Research Station, Building Research Establishment, Borehamwood, Herts, UK.

Heskestad, G. 1988. Fire Plumes, SFPE Handbook of Fire Protection Engineering, Society of Fire Protection Engineers, Boston, MA.

Heskestad, G. 1984. Engineering Relations for Fire Plumes, Fire Safety Journal, Vol 7, No 1, pp 25-32.

Heskestad, G. 1986. Fire Plume Air Entrainment According to two Competing Assumptions, Twenty-first Symposium (International) on Combustion, Combustion Institute, Pittsburgh, PA, pp 111-120.

Heskestad, G. 1989. Inflow of Air Required at Wall and Ceiling Apertures to Prevent Escape of Fire Smoke, FMRC J.I. OQ4E4.RU, Norwood, MA, Factory Mutual Research Corporation.

Heskestad, G. 1983. Virtual Origins of Fire Plumes, Fire Safety Journal, Vol 5, No 2, pp 109-114.

Heskestad, G. 1991. Letter to the Editor, Fire Technology, Vol 27, No 2, pp 174-185.

Jones, W.W. 1983. A Review of Compartment Fire Models, Nat. Bur. of Stand. (U.S.), NBSIR 83-2684.

Klote, J.H. 1990. Fire Experiments of Zoned Smoke Control at the Plaza Hotel in Washington DC, ASHRAE Transactions, Vol 96, Part 2.

Klote, J.K. and Milke, J.A. 1992. Design of Smoke Management Systems, American Society of Heating, Refrigerating and Air-conditioning Engineers, Atlanta, GA.

Law, M. 1982. Air-Supported Structures: Fire and Smoke Hazards, Fire Prevention, Vol 148, pp 24-28.

Lui, S.T. 1977. Analytical and Experimental Study of Evaporative Cooling and Room Fire Suppression by Corridor Sprinkler System, National Bureau of Standards, NBSIR 77-1287.

Madrzykowski, D. 1991. The Reduction in Fire Hazard in Corridors and Areas Adjoining Corridors Provided by Sprinklers, National Institute of Standards and Technology, NISTIR 4631.

Mawhinney, J.R. and Tamura, G.T. 1994. Effect of Automatic Sprinkler Protection on Smoke Control Systems, ASHRAE Transactions, Vol 100, Part 1.

McCaffrey, B.J., Quintiere, J.G. and Harkleroad, M.F. 1981. Estimating Room Temperature and the Likelihood of Flashover Using Fire Test Data Correlations, Fire Technology, Vol 17, No 2, p 98.

McCaffrey, B.J. 1983. Momentum Implications for Buoyant Diffusion Flames, Combustion and Flame, Vol 52, No 2, pp 149-167.

McCoubrey, A.O. 1991. Guide for the Use of the International System of Units - The Modernized Metric System, National Institute of Standards and Technology, NIST Special publication 811.

Milke, J.A. and Mower, F.W. 1994. Computer-Aided Design for Smoke Management in Atria and Covered Malls, ASHRAE Transactions, Vol 100, Part 2.

Mitler, H.E. 1984. Zone Modeling of Forced Ventilation Fires, Combust. Sci. Tech., Vol 39, pp 83-106.

Mitler, H.E. and Rockett, J.A. 1986. How Accurate is Mathematical Fire Modeling?, Nat. Bur. Stand. (U. S.), NBSIR 86-3459.

Mitler, H.E. and Emmons, H.W. 1981. Documentation for CFC V, the fifth Harvard computer code. Home Fire Project Tech. Rep. #45, Harvard University.

Morgan, H.P. 1979. Smoke Control Methods in Enclosed Shopping Complexes of One or More Stories: A Design Summary, Fire Research Station, Borehamwood, Herts, UK.

Morgan, H.P. and Hansell, G.O. 1987. Atrium Buildings: Calculating Smoke Flows in Atria for Smoke Control Design, Fire Safety Journal, Vol 12, pp 9-12.

Morton, B.R., Taylor, G., and Turner, J.S. 1956. Turbulent Gravitational Convection from Maintained and Instantaneous Sources, Proceedings of the Royal Society of London, Vol 234, pp 1-23.

Nelson, H.E. and MacLennan, H.A. 1988. Emergency Movement, SFPE Handbook of Fire Protection Engineering, Society of Fire Protection Engineers, Boston, MA.

NFPA 92B 1991. Guide for Smoke Management Systems in Malls, Atria, and Large Areas, National Fire Protection Association, Quincy, MA.

NFPA 92A 1993. Recommended Practice for Smoke Control Systems, National Fire Protection Association, Quincy, MA.

Notarianni, K.A. and Davis, W.D. 1993. The Use of Computer Models to Predict Temperature and Smoke Movement in High Bay Spaces, National Institute of Standards and Technology, NISTIR 5304.

Pauls, J. 1988. People Movement, SFPE Handbook of Fire Protection Engineering, Society of Fire Protection Engineers, Boston, MA.

Peacock, R.D., Forney, G.P., Reneke, P., Portier, R. and Jones, W.W. 1993. CFAST, the Consolidated Model of Fire Growth and Smoke Transport, National Institute of Standards and Technology, NIST Technical Note 1299.

Peacock, R.D., Jones, W.W., Bukowski, R.W., and Forney, C.L. 1991. Software User's Guide for HAZARD I, Version 1.1, NIST Handbook 146, Vol I, National Institute of Standards and Technology, Gaithersburg, MD.

Quintiere, J.G. 1989. Fundamentals of Enclosure Fire "Zone" Models, Journal of Fire Protection Engineering, Vol 1, No 3, pp 99-119.

Tanaka, T. 1983. A Model of Multiroom Fire Spread. Nat. Bur. of Stand. (U.S.), NBSIR 83-2718.

Thomas, I. 1990. Progress in Australia Towards Engineering Design for Fire Safety in Buildings, NIST Fire Research Video R9100911.

UBC 1993. Accumulative Supplement to the Uniform Building Code, International Conference of Building Officials, Whittier, CA.

Walton, W.D. and Notarianni, K.A. 1993. A Comparison of Ceiling Jet Temperatures Measured in an Aircraft Hanger Test Fire with Temperatures Predicted by the DETACT_QS and LAVENT Computer Models, National Institute of Standards and Technology, NISTIR 4947.

Walton, W.D. 1985. ASET-B: A Room Fire Program for Personal Computers, National Bureau of Standards, NBSIR 85-3144-1.

Appendix A Bibliography

Adiga, K.C., Ramaker, D.E., Tatem, P.A., Williams, F.W. 1985. Field Modeling Approach for Fires Over Large Liquid Pools: Boundary Layer Combustion Analysis. Proceedings. Combustion Institute/Eastern States Section. Chemical and Physical Processes in Combustion. Fall Technical Meeting, November 4-6, 1985, Philadelphia, PA.

Bagnaro, M., Laouisset, M., Lockwood, F.C. 1983. Field Model Prediction of Some Room Fires: Steady and Transient. (Proceedings) , American Society of Mechanical Engineers. Fire Dynamics and Heat Transfer. 21st National Heat Transfer Conference. July 24-28, 1983., HTD-Vol 25, Seattle, Wa, American Society of Mechanical Engineers, New York, Quintiere, J.G., Alpert, R.L. and Altenkirch, R.A. Editor(s), pp 107-114.

Baum, H.R. and Rehm, R.G. 1984. Finite Difference Solutions for Internal Waves in Enclosures. SIAM J. Scientific and Statistical Computing, Vol 5, No 4, pp 958-977.

Baum, H.R., Rehm, R.G., Barnett, P.D., Corley, D.M. 1983. Finite Difference Calculation of Buoyant Convection in an Enclosure Part 1. The Basic Algorithm. SIAM Journal on Scientific and Statistical Computing, Vol 4, No 1, pp 117-135.

Baum, H.R. 1976. Analysis of Turbulent Mixing Layers Using a Two Equation Model of Turbulence. U. S./Japan Government Cooperative Program on Natural Resources. Panel on Fire Research and Safety. Volume 5. Fire Modeling. October 19-22, 1976, Tokyo, Japan, pp 1-45.

Baum, H.R. and Rehm, R.G. 1988. Transient Combustion in a Turbulent Fire. Proceedings. National Bureau of Standards, NBSIR 88-3753.

Beier, R.A., de Ris, J. and Baum, H. 1982. Accuracy of Finite Difference Methods in Recirculating Flows. Factory Mutual Research Corp., Norwood, MA.

Beyler, C., 1986. Fire Plumes and Ceiling Jets, Fire Safety J., 11, July/September, p. 53-76.

Chambers, T.L., Wilcox, D.C. 1976. A Critical Examination of Two-Equation Turbulence Closure Models, AIAA Paper 76-352, San Diego, CA.

Chow, W.K. 1993. Simulation of the Atrium Fire Environment in Hong Kong, ASHRAE Transactions, Vol 99, Part 2.

Cooper, L.Y., Harkleroad, M., Quintiere, J. and Rinkinen, W., 1981. An Experimental Study of Upper Hot Layer Stratification in Full-Scale Multiroom Fire Scenarios, Paper 81-HT-9, The American Society of Mechanical Engineers.

Cox, G. 1987. UK Fire Research Station Field Modeling Activities, CIB W14 Workshop on Fire Modelling - March 16 - 17, 1990, Berlin, CIB Publication 104.

Cox, G., Kumar, S. and Markatos, N. C. 1985. Some Field Model Validation Studies. International Association for Fire Safety Science. Fire Safety Science. 1st International Symposium. October 7-11, 1985.

Cox, G., Kumar, S., Cumber, P. and Thomson, V. 1990. Fire Simulation in the Design Process: An Exemplification of the use of a Computer Field Model.

Cox, G. 1987. UK Fire Research Station Field Modeling Activities, CIB W14 Workshop on Fire Modeling. March 1987, CIB Publication 104, Berlin, West Germany, p 5.

Cox, G., Chitty, R. and Kumar, S. 1989. Fire Modelling and the King's Cross Fire Investigation. Letter to the Editor. Journal. Fire Safety Journal, Vol 15, No 1, pp 103-106.

Cox, G. and Kumar, S. 1983. Computer Modelling of Fire. Report. Fire Research Station, Borehamwood, England.

Cox, G. and Kumar, S. 1987. Field Modelling of Fire in Forced Ventilated Enclosures, Combustion Science and Technology, Vol 52, No 1, pp 7-23.

Cox, G. 1983. Field Model of Fire and Its Application to Nuclear Containment Problems. CSNI Specialist Meeting on Interaction of Fire and Explosion With Ventilation Systems in Nuclear Facilities. April 25-28, 1983., Los Alamos, NM, pp 199-210.

Cox, G. 1987. Simulating Fires in Buildings by Computer--The State of the Art. Journal of the Forensic Science Society, Vol 27, pp 175-188.

Cox, G. 1984. Simulating Fires in Buildings by Computer - The State of the Art. 10th International Assoc. of Forensic Sciences Meeting, Oxford.

Cox, G. 1985. Mathematical Modelling of Fires in Enclosures. International Conference on Flammability. INTERFLAM '85. March 26-28, 1985., Guildford, England, pp 56-63.

Cox, G. 1985. Fighting Fire in the Computer. Journal. Spectrum, No 191, pp 8-10.

Daly, B.J. and Harlow, F.H. 1970. Transport Equations in Turbulence, Phys. Fluids, Vol 13, pp 2634-2649.

Davis, W.D. and Cooper, L.Y. 1989. Estimating the Environment and the Sprinkler Links in Compartment Fires With Draft Curtains and Fusible-Link-Actuated Ceiling Vents - Part II: User Guide for the Computer Code LAVENT, National Institute of Standards and Technology, NISTIR 89-4122.

Davis, W.D. and Cooper, L.Y. 1991. A Computer Model for Estimating the Response of Sprinkler Links to Compartment Fires With Draft Curtains and Fusible Actuated Ceiling Vents, Fire Technology, Vol 27, No 2, pp 113-127.

DeCicco, P.R. and Cresci, R.J. 1975. Smoke and Fire Control in Large Atrium Spaces, ASHRAE Transactions, Vol 81, Part 2, pp 319-335.

Emmons, H.W. 1985. Needed Fire Science. Report. Harvard University. Home Fire Proj. Tech. Rpt. 66

Fusegi, T., Farouk, B., Hyun, J.M. and Kuwahara, K. 1990. A Direct Numerical Simulation of Natural Convection in a Differentially Heated Cubical Enclosure. International Symp. on Engineering Turbulence Modelling & Measurements, Sept. 24-28, 1990, Dubrovnik, Yugoslavia.

Galea, E. 1989. On the Field Modelling Approach to the Simulation of Enclosure Fires. Journal of Fire Protection Engineering, Vol 1, No 1, pp 11-22.

Galea, E. 1989. On the Field Modelling Approach to the Simulation of Enclosure Fires, Journal of Fire Protection Engineering, Vol 1, No 1, pp 11-22.

Hadjisophocleous, G.V. and Cacambouras, M. 1993. Computer Modeling of Compartment Fires, Journal of Fire Protection Engineers, Vol 5, No 2, pp 39-52.

Hanjalic, K. and Launder, B.E. 1972. A Reynolds Stress Model of Turbulence and Its Application to Asymmetric Shear Flows, Journal of Fluid Mechanics, Vol 52, pp 609-638.

Hansell, G.O., and Morgan, H.P. 1988. Smoke Control in Atrium Buildings Using Depressurization, PD 66/88, Borehamwood, Fire Research Station.

Hansell, G.O., and Morgan, H.P. 1994. Design Approaches for Smoke Control in Atrium Buildings, BR 258, Fire Research Station, Borehamwood, Herts, UK.

Hasemi, Y. 1976. Numerical Simulation of the Natural Convection in Fire Compartment, 2nd Joint Meeting US. Japan Panel on Fire Safety, UJNR, Tokyo.

Heselden, A.J.M. 1970. Smoke travel in shopping malls experiments in co-operation with Glasgow Fire Brigade - Part 2, F.R. Note No 854, Fire Research Station, Borehamwood, Herts, UK.

Heselden, A.J.M. and Hinkley, P.L. 1970. Smoke travel in shopping malls experiments in co-operation with Glasgow Fire Brigade - Part 1, F.R. Note No 832, Fire Research Station, Borehamwood, Herts, UK.

Heskestad, G. and Delichatsios, M.A. 1977. Environments of Fire Detectors - Phase I: Effect of Fire Size, Ceiling Height and Materials. Volume I - Measurements (NBS-GCR-77-86), Volume II - Analysis (NBS-GCR-77-95), Gaithersburg, MD, National Bureau of Standards.

Heskestad, G. 1989. Note on Maximum Rise of Fire Plumes in Temperature-Stratified Ambients, Fire Safety Journal, Vol 15, pp 271-276.

Hinkley, P.L. 1970. The flow of hot gases along an enclosed shopping mall, F.R. Note No 807, Fire Research Station, Borehamwood, Herts, UK.

Hinkley, P.L. 1970. A Preliminary Note on the Movement of Smoke in an Enclosed Shopping Mall, Fire Research Note 806, Fire Research Station, Borehamwood, U.K.

Honig, M.L. 1987. Use of a Field Model in Fire-Engineering, CIB W14 Workshop on Fire Modelling - March 16 - 17, 1990, Berlin, CIB Publication 104.

Honig, M.L. 1987. Use of a Field Model in Fire Engineering. Proceedings.CIB W14 Workshop on Fire Modeling. March 1987, Berlin, West Germany.

Houck, R.R. 1988. Numerical Field Model Simulation of Full-Scale Fire Tests in a Closed Spherical/Cylindrical Vessel With Internal Ventilation. Thesis.

Jackson, L. 1988. Modelling the Future by Computer. Fire Prevention, No 215, pp 34-35.

Jones, W.P. and Launder, B.E. 1972. The Prediction of Laminarization with a Two-Equation Model of Turbulence, International Journal of Heat and Mass Transfer, Vol 15, pp 301-314.

Kawagoe, K. and Morita, M. 1987. Mathematical Modeling in Japan. CIB W14 Workshop on Fire Modeling, Berlin.

Keski-Rahkonen, O. 1987. Numerical Fire Simulation in Finland. CIB W14 Workshop on Fire Modelling, Berlin.

Kumar, S. and Cox, G. 1989. Radiation and Surface Roughness Effects in the Numerical Modelling of Enclosure Fires. Proceedings. International Association for Fire Safety Science. Fire Safety Science. Proceedings. 2nd International Symposium. June 13-17, 1988, Tokyo.

Kumar, S. 1983. Mathematical Modelling of Natural Convection in Fire--A State of the Art Review of the Field Modelling of Variable Density Turbulent Flow. Fire and Materials, Vol 7, No 1, pp 1-24.

Kumar, S. and Cox, G. 1985. Mathematical Modelling of Fires in Road Tunnels. Aerodynamics and Ventilation of Vehicle Tunnels, 5th International Symposium.

Kurabuchi, T., Fang, J.B. and Grot, R.A. 1990. A Numerical Method for Calculation Indoor Airflows Using a Turbulence Model, National Institute of Standards and Technology, NISTIR 89-4211.

Launder, B.E. 1979. Stress-Transport Closures: Into the Third Generation, Proc. First Symposium on Turbulent Shear Flows, Springer-Verlag, New York.

Launder, B.E. and Spalding, D.B. 1974. The Numerical Computation of Turbulent Flows, Computer Methods in Applied Mechanics and Engineering, Vol 3, pp 269-289.

Lockwood, F.C. and Malalasekera, W.M.G. 1989. Fire Computation: The 'Flashover' Phenomenon, Combustion Institute, Symposium on Combustion, 22nd. August 14-19, 1988, Seattle, WA, Combustion Institute, Pittsburgh, PA, pp 1319-1328.

Markatos, N.C. and Pericleous, K.A. 1983. Investigation of Three Dimensional Fires in Enclosures. American Society of Mechanical Engineering. National Heat Transfer Conference, 21st. July 24-28, 1983., Seattle, WA, ASME, New York, NY, Quintiere, J.G., Alpert, R.L. and Altenkirch, R.A., Editor(s), pp 115-124.

Markatos, N.C., Pericleous, K.A. and Cox, G. 1986. Novel Approach to the Field Modelling of Fire. Physico Chemical Hydrodynamics, Vol 7, No 2, pp 125-143.

Markatos, N.C. and Cox, G. 1984. Hydrodynamics and Heat Transfer in Enclosures Containing a Fire PCH Physiochemical Hydrodynamics, Vol 5, No 1, pp 53-66.

McGrail, D.M. Denver's Polo Club Condo Fire: Atrium Turns High-Rise Chimney, Fire Engineering, pp 67-74.

Milke, J.A. and Mowrer, W.M. 1993. A Design Algorithm for Smoke Management Systems in Atria and Covered Malls, Report No FP93-04, University of Maryland, College Park, MD.

Modak, A.T., and Alpert, R.L. 1982. Influence of Enclosures on Fire Growth - Volume I: Guide to Test Data, FMRC OAOR2.BU-8, Norwood, MA, Factory Mutual Research.

Morgan, H.P. and Marshall, N.R. 1978. Smoke Hazards in Covered, Multi-Level Shopping Malls: A Method of Extracting Smoke from Each Level Separately, Building Research Establishment, Borehamwood, U.K.

Morgan, H.P. and Hansell, G.O. 1987. Atrium Buildings: Calculating Smoke Flows in atria for Smoke-control Design, Fire Safety Journal, Vol 12(1987), pp 9-35.

Morgan, H.P. and Gardner, J.P. 1990. Design Principles for Smoke Ventilation in Enclosed Shopping Centres, BR 186, Fire Research Station, Borehamwood, Herts, UK.

Morgan, H.P., Marshall, N.R. and Gladstone, B.M. 1976. Smoke Hazards in Covered Multi-Level Shopping Malls: Smoke Studies Using a Model 2-Story Mall, Building Research Establishment, Borehamwood, U.K.

Morgan, H.P. and Marshall, N.R. 1975. Smoke Hazards in Covered, Multi-Level Shopping Malls: An Experimentally-Based Theory for Smoke Production, Building Research Establishment, Borehamwood, U.K.

Moss, J.B., Cox, G. and Kumar, S. 1987. Laminar Flamelet Models of Fire - the Prospect. CIB W14 Workshop on Fire Modeling, Berlin, Mar 1987, CIB Publication 104.

Mulholland, G., Handa, T., Sugawa, O. and Yamamoto, H. 1981. Smoke Filling in an Enclosure, Paper 81-HT-8, The American Society of Mechanical Engineers.

Nelson, H.E. 1987. An Engineering Analysis of the Early Stages of Fire Development - The Fire at the Dupont Plaza Hotel and Casino - December 31, 1986, National Institute of Standards and Technology, NISTIR 87-3560.

Ng, K.H. and Spalding, D.B. 1972. Turbulence Model for Boundary Layers Near Walls, Physics of Fluids, Vol 15, pp 20-30.

Pericleous, K.A., Worthington, D.R.E. and Cox, G. 1989. Field Modelling of Fire in an Air-Supported Structure. International Association for Fire Safety Science. Fire Safety Science. 2nd International Symposium. June 13-17, 1988, Tokyo.

Phillips, A.M. 1971. Smoke travel in shopping malls model studies - Part 1: rates of lateral spread, F.R. Note No 864, Fire Research Station, Borehamwood, Herts, UK.

Quintiere, J. 1984. Perspective on Compartment Fire Growth. Combustion Science and Technology, Vol 39, No 1, pp 11-54.

Rehm, R.G., Baum, H.R., Barnett, P.D. and Corley, D.M. 1984. Finite Difference Calculations of Buoyant Convection in an Enclosure. Part 2: Verification of the Nonlinear Algorithm. Final Report. National Bureau of Standards, Gaithersburg, MD. NBSIR 84-2932.

Rehm, R.G., Barnett, P.D., Baum, H.R. and Corley, D.M. 1985. Finite Difference Calculations of Buoyant Convection in an Enclosure: Verification of the Nonlinear Algorithm. Applied Numerical Mathematics, Vol 1, pp 515-529.

Rehm, R.G., Baum, H.R., Barnett, P.D., Sweet, R.A., O'Leary, D.P. and Corley, D.M. 1982. Three Dimensional Computations of Fire Induced Flow--A Preliminary Report. Combustion Institute/Eastern States Section. December 14-16, 1982, Atlantic City, NJ.

Reinhardt, H.J. 1987. Field Model for Postcalculations by COBRA-NC of the HDR-Fire-Experiments T51.2. CIB W14 Workshop on Fire Modeling. March 1987, CIB Publication 104, Berlin, West Germany.

Rubesin, M.W. 1977. Numerical Turbulence Modeling, AGARD Lecture Series No 86 on Computational Fluid Dynamics, pp. 3-1 to 3-37.

Saffman, P.G. and Wilcox, D.C. 1974. Turbulence Model Predictions for Turbulent Boundary Layers, AIAA J., Vol 12, pp 541-546.

Wilcox, D.C. and Traci, R.M. 1976. A Complete Model of Turbulence, AIAA Paper 76-351, San Diego, CA.

Williamson, B. and Mowrer, F. 1987. A Method to Characterize Heat Release Rate Data from Large-Scale Experiments, presented at the Eastern States Section of the Combustion Institute, Gaithersburg MD.

Wolfstein, M. 1969. The Velocity and Temperature Distribution in One-dimensional Flow with Turbulence Augmentation and Pressure Gradient, International Journal of Heat and Mass Transfer, Vol 12, pp 301-318.

Yoshikawa, T., Mashigh, J., Jo, T. and Sugawa, O. 1987. Numerical Simulation of Early Stage of a Compartment Fire by Field Model. 9th Joint Panel Meeting of the UJNR Panel.

Zukoski, E.E. and Kubota, T. 1980. Tow-layer modeling of smoke movement in building fires, Fire and Materials, Vol 4, No 17.

Appendix B Unit Systems and Physical Data

Physical quantities such as length, weight, and time are expressed in terms of standard units of measurement. In this paper, both international system (SI) units and English units are used.

Newton's second law of motion states that the force, F, on a body of fixed mass, m, is proportional to the product of the mass and the acceleration, a.

$$F \propto m\,a \tag{B28}$$

The SI system has advantages with regard to equation derivation and calculations over the English unit systems. There are three common English unit systems with regard to mass and force: the pound mass and pound force system, the slug and pound system, and the pound mass and poundal system. Introduction of the proportionality constant $1/g_c$ into the above relation yields

$$F = \frac{m\,a}{g_c} \tag{B29}$$

Table B.1 lists the units for these systems and the SI system along with the values of g_c for each. Generally, a pound is thought of as a unit of force. However, in some engineering applications, the pound also has been used as a unit of mass. One pound mass (lbm) is the mass of a body that weighs one pound (lb) at sea level. One slug equals 32.174 lbm, and one poundal is a force of 0.03108 pounds. For the systems listed in table B.1 for which the value of g_c is one, Newton' second law can be written as

$$F = m\,a \tag{B30}$$

This formulation of Newton's law simplifies derived equations and calculations, and unit systems that satisfy this equation will be referred to here as *dimensionlly homogeneous*. This homogeneity is accomplished by defining one of the four units (length, mass, time and force) in terms of the other three. Thus three of the units become base units and the other is a derived unit. Theoretically, any three can be selected as base units.

In the SI system, the unit of force is the newton, N, which is the force required to accelerate a mass of one kilogram at a rate of one meter per second squared. Because force is a derived unit in the SI system, that convention is used in the following discussion for the English system. The unit of mass in the English system will be taken to be the slug. A slug can be thought of as a mass that has a weight of 32.174 pounds at sea level. In the English system, the unit of force is the pound, lb, which is the force required to accelerate a mass of one slug at a rate of one foot per second squared.

The base units and derived unit discussed above relate force and mass, but many more units are needed for engineering calculations. The base units and derived units needed for smoke control applications are

listed in tables B.2 and B.3. In the SI system, prefixes are used to form decimal multiples and submultiples of the SI units. The SI prefixes are listed in table B.4. The conversion factors listed in Table B.5 have been rounded off to three or four significant figures, which is sufficient for most smoke management calculations.

Absolute temperature is measured in the Kelvin scale in the SI system and the Rankine scale in the English system. In addition, temperature is frequently measured in the Celsius or the Fahrenheit scale. The equations below relate these temperature scales.

$$
\begin{aligned}
T_K &= T_R/1.8 \\
T_K &= (T_F + 459.67)/1.8 \\
T_K &= T_C + 273.15 \\
T_C &= (T_F - 32)/1.8 \\
T_C &= T_K - 273.15 \\
T_C &= T_R/1.8 - 273.15 \\
T_R &= T_F + 459.67 \\
T_R &= 1.8(T_C + 273.15) \\
T_R &= 1.8T_K \\
T_F &= 1.8T_K - 459.67 \\
T_F &= 1.8T_C + 32 \\
T_F &= T_R - 459.67
\end{aligned}
\qquad \text{(B31)}
$$

where

T_K = temperature in the kelvin scale
T_C = temperature in degrees Celsius
T_R = temperature in degrees Rankine
T_F = temperature in degrees Fahrenheit

For further information concerning the SI system, the reader is referred to McCoubrey (1991).

Table B.1 Units relating force and mass in various systems

Quantity	International System (SI)	Slug & Pound	Pound Mass & Poundal	Pound Mass & Pound Force
length	meter (m)	foot (ft)	foot (ft)	foot (ft)
time	second (s)	second (sec)	second (sec)	second (sec)
mass	kilogram (kg)	slug	pound mass (lbm)	pound mass (lbm)
force	Newton (N)	pound (lb)	poundal	pound force (lbf)
g_c	1 kg m/ N s^2	1 slug ft/ lbf sec^2	1 lbm ft/ poundal sec^2	32.174 lbm ft/ lbf sec^2

Table B.2 Base units of SI System

Quantity	Unit	Symbol
length	meter	m
mass	kilogram	kg
time	second	s
thermodynamic (absolute) temperature	kelvin	K

Table B.3 Derived units of SI System

Quantity	Unit	Symbol	Formula
force	newton	N	$kg \cdot m/s^2$
pressure	pascal	Pa	N/m^2
energy, work or heat	joule	J	$N \cdot m$
power, heat release rate	watt	W	J/s

Table B.4 Some SI prefixes

Prefix	Symbol	Multiplication Factor
giga	G	$10^9 = 1\ 000\ 000\ 000$
mega	M	$10^6 = 1\ 000\ 000$
kilo	k	$10^3 = 1\ 000$
centi	c	$10^{-2} = 0.01$
millii	m	$10^{-3} = 0.001$
micro	μ	$10^{-6} = 0.000\ 001$
nano	n	$10^{-9} = 0.000\ 000\ 001$

Table B.5 Factors for conversion to SI units

Multiply	By	To Obtain
Btu	1055	J
Btu/s	1055	W
Btu/hr	0.293	W
foot (ft)	0.3048	m
ft^2	0.0929	m^2
ft^3/min (cfm)	4.72×10^{-4}	m^3/s
ft^3/min (cfm)	0.472	L^*/s
inch (in)	0.0254	m
pound mass (lbm)	0.454	kg
pound force (lbf)	4.445	N
pound per square inch (psi)	6895.	Pa

Table B.6 Physical Constants

acceleration of gravity at sea level, g	9.80665 m/s^2
	32.174 ft/sec^2
gas constant of air, R	287.0 J/kg K
	53.34 ft lbf/lbm °R
standard atmospheric pressure, P	101325 Pa
	14.696 psi
	2116. lbf/ft^2

Appendix C ASMET Description

Nomenclature

A = cross-sectional area of the atrium, m^2
a = fire growth coefficient, kW/s^2
C_1 = 0.071
C_2 = 0.026
C_3 = 0.083
C_4 = 1
C_5 = 9.1
C_7 = 0.235
C_8 = 0.0018
C_9 = 0.166
C_{10} = 1.11
C_{11} = 0.91
C_{12} = 0.937
C_p = specific heat of plume gases, 1.005 kJ/kg K
D_f = diameter of fire, m
g = acceleration of gravity, 9.807 m/s^2
H = ceiling height above the fire, ft (m);
$\dot{m}$ = mass flow in plume at height z, kg/s
P = absolute pressure, Pa
Q = heat release of the fire, kW
Q_c = convective heat release rate of fire, kW
R = gas constant, 287 J/kg K
t = time, s
T = absolute temperature, K
T_a = ambient temperature, °C
T_{cp} = absolute centerline plume temperature at elevation z, K
t_g = growth time, s
T_p = average plume temperature at elevation z, °C
T_p = average plume temperature at elevation z, °C
$\dot{V}$ = volumetric smoke flow at elevation z, m^3/s
z = height above top of fuel, m
z_f = mean flame height, m
z_o = virtual origin of the plume, m
ξ = convective fraction of heat release
ρ = density of air or plume gases, kg/m^3
ρ_a = density of ambient air, kg/m^3
ρ_p = density of plume gases at elevation z, kg/m^3

Note: The variable above are given in SI units only, because internal calculations in ASMET are SI.

Below are the equations used in each section of ASMET, except for ASET-C which is discussed in Appendix E.

1. Steady Filling Equation (Solve for z)

$$\frac{z}{H} = C_{10} - 0.28 \ln\left(\frac{t\,Q^{1/3}\,H^{-4/3}}{\frac{A}{H^2}}\right) \tag{C32}$$

2. Steady Filling Equation (Solve for t)

$$t = \frac{A}{H^2}\,\frac{H^{4/3}}{Q^{1/3}} \exp\left[\frac{1}{0.28}\left(C_{10} - \frac{z}{H}\right)\right] \tag{C33}$$

3. Unsteady Filling Equation (Solve for z)

$$\frac{z}{H} = C_{11}\left[t\,t_g^{-2/5}\,H^{-4/5}\left(\frac{A}{H^2}\right)^{-3/5}\right]^{-1.45} \tag{C34}$$

4. Unsteady Filling Equation (Solve for t)

$$t = C_{12}\,t_g^{2/5}\,H^{4/5}\left(\frac{A}{H^2}\right)^{3/5}\left(\frac{z}{H}\right)^{-0.69} \tag{C35}$$

5. Simple Plume Equations

Mass flow of plume:

$$\dot{m} = C_1 Q_c^{1/3} z^{5/3} + C_8 Q_c \tag{C36}$$

Mean flame height:

$$z_f = C_9 Q_c^{2/5} \tag{C37}$$

Average plume temperature:

$$T_p = T_a + \frac{Q_c}{\dot{m} C_p} \tag{C38}$$

The volumetric flow of a plume:

$$\dot{V} = C_4 \frac{\dot{m}}{\rho_p} \tag{C39}$$

The density of air and plume gases:

$$\rho = \frac{p}{R T} \tag{C40}$$

6. Plume With Virtual Origin Correction

Mass flow of plume:

$$\dot{m} = C_1 Q_c^{1/3} (z - z_o)^{5/3} \left[1 + C_2 Q_c^{2/3} (z - z_o)^{-5/3}\right] \tag{C41}$$

This equation can be rearranged to simplify calculation:

$$\dot{m} = C_1 Q_c^{1/3} (z - z_o)^{5/3} + C_8 Q_c \tag{C42}$$

Virtual origin of the plume:

$$z_o = C_3 Q^{2/5} - 1.02 D_f \tag{C43}$$

Mean flame height:

$$z_f = C_7 Q^{2/5} - 1.02 D_f \tag{C44}$$

Average plume temperature:

The volumetric flow of a plume:

$$T_p = T_a + \frac{Q_c}{\dot{m} C_p} \tag{C45}$$

$$\dot{V} = C_4 \frac{\dot{m}}{\rho_p} \tag{C46}$$

The density of air and plume gases:

$$\rho = \frac{p}{R T} \tag{C47}$$

7. Plume Centerline Temperature

Plume Centerline Temperature:

$$T_{cp} = T_a + C_5 \left(\frac{T_a}{g C_p^2 \rho^2} \right)^{1/3} \frac{Q_c^{2/3}}{(z - z_o)^{5/3}} \tag{C48}$$

The virtual origin of the plume and the mean flame height by the equations of the previous section.

Convective portion of the heat release rate:

$$Q_c = \xi Q \tag{C49}$$

The convective fraction, ξ, is generally taken as 0.7 for design. However, when burning a known fuel (as in acceptance testing), it may be desired to use the specific value for the fuel.

Appendix D ASMET Users Guide

ASMET is a collection of tools that can be used for analysis of atria smoke management systems. This program is for a Personal Computer with a DOS operating system, and the program was written in C. When ASMET is in the active directory, the program is activated by typing **ASMET** followed by pressing the <Enter> key. When the program starts, the main menu appears on the screen as shown in table D1.

Table D.1 Main menu screen of ASMET

```
ASMET: Atria Smoke Management Engineering Tools

                    Menu

   Steady Filling Equation (Solve for z)
   Steady Filling Equation (Solve for t)
   Unsteady Filling Equation (Solve for z)
   Unsteady Filling Equation (Solve for t)
   Simple Plume Equation
   Plume With Virtual Origin Correction
   Plume Centerline Temperature
   ASET-C (C language version of ASET-B)
   Input units (SI or English): SI
   Exit
```

The equations used for each routine are listed in Appendix C, except for ASET-C which is described in Appendix E. The equations of Appendix C are also addressed in the in the body of the text.

The first time the program is run, it starts in SI units, and the user can change units by pressing **E** for English units or **I** for SI units. The program stores a unit indicator in file UNITS so that it will start up with the unit selection from that last time the program was run. The other menu items are selected by pressing the key that is in bold type (or yellow on a color monitor).

The first menu item is selected by pressing **S**, and the screen for this menu is shown in table D2. There are two ways to enter data from this menu. The first is by pressing the key that is in bold for that menu item. The second is by moving the indicator at the right of the menu item with the up and down arrows. This indicator is next to the first menu item (ceiling height above fire) in figure D2. Once an item has been selected, the number for that item is entered followed by <Enter>. Table D3 shows the screen after data has been entered.

The data displayed on the screen can be sent to the printer by pressing **P**, and pressing **D** returns to user to the main menu. To send results to a file, press **f** and enter the file name. Use of the other items in the main menu is similar to that discussed above.

Table D2. Screen for steady filling equation (solve for z)

```
                    Steady smoke filling

  Height of smoke layer during atrium filling from a steady fire

   ceiling height above fire       H (m):
   cross-sectional area of atrium  A (m^2):
   heat release rate of fire       Q (kW):
   time                            t (s):
   Print results (to LPT1)
   Print results to file disabled
   Done (return to main menu)
```

Table D3. Screen for steady filling equation after data is entered

```
                    Steady smoke filling

  Height of smoke layer during atrium filling from a steady fire

   ceiling height above fire       H (m):       80.00
   cross-sectional area of atrium  A (m^2):  20000.00
   heat release rate of fire       Q (kW):   10000.00
   time                            t (s):     1200.00
   Print results (to LPT1)
   Print results to file disabled
   Done (return to main menu)



  Height of smoke layer above fire, z, is     17.6 m  or    57.8 ft
```

Example Output (SI Units)

Steady Filling Equation (Solve for z)

Height of smoke layer during atrium filling from a steady fire

ceiling height above fire	H (m):	30.00
cross-sectional area of atrium	A (m^2):	5000.00
heat release rate of fire	Q (kW):	5000.00
time	t (s):	200.00

Height of smoke layer above fire, z is 17.4 m or 57.2 ft

Steady Filling Equation (Solve for t)

Atrium filling time for steady fire

ceiling height above fire	H (m):	40.00
cross-sectional area of atrium	A (m^2):	10000.00
heat release rate of fire	Q (kW):	5000.00
height of smoke layer above fire	z (m):	8.00

Filling time is 1290 seconds or 21.5 min.

Unsteady Filling Equation (Solve for z)

Atrium filling time for unsteady fire

ceiling height above fire	H (m):	30.00
cross-sectional area of atrium	A (m^2):	8000.00
fire growth constant (Menu)	a (kW/s^2):	0.04689
time	t (s):	800.00

At 800 seconds, the fire is 30010 kW or 28445 Btu/s.

Height of smoke layer above fire, z is 10.7 m or 35.0 ft

Example Output (SI Units) Continued

Unsteady Filling Equation (Solve for t)

Atrium filling time for unsteady fire

ceiling height above fire	H (m):	50.00
cross-sectional area of atrium	A (m^2):	12000.00
fire growth constant (Menu)	a (kW/s^2):	0.04689
height of smoke layer above fire	z (m)	10.00

Filling time is 1237 seconds or 20.6 min.
At this time, the fire is 71754 kW or 68014 Btu/s.

Simple plume equation

mass flow and temperature rise of an plume

without correction for virtual origin

Elevation	z (m):	50.00
Heat release rate of fire	Q (kW):	25000.00
Ambient temperature	Ta (C):	21.00

At elevation z, the plume has:

Mass flow of	1282.4 kg/s	2827.2 lb/s
Volumetric flow of	1117.2 m^3/s	2367016 cfm
Average temperature of	35 C	94 F
Mean flame height of	8.3 m	27.1 ft

Example Output (SI Units) Continued

Plume With Virtual Origin Correction

Mass flow rate and average plume temperature

Elevation	z (m):	50.00
Heat release rate of fire	Q (kW):	25000.00
fire diameter	Df (m):	4.00
Ambient temperature	Ta (C):	21.00

At elevation z, the plume has:

Mass flow of	1254.7	kg/s	2766.1	lb/s
Volumetric flow of	1094.2	m^3/s	2318122	cfm
Average temperature of	35	C	95	F
Virtual origin at	0.7	m	2.3	ft
Mean flame height of	9.4	m	30.9	ft

Plume Centerline Temperature

calculate centerline plume temperature

Elevation	z (m):	50.00
Heat release rate of fire	Q (kW):	25000.00
fire diameter	Df (m):	4.00
Convective fraction of heat release	(0.6 to 1):	0.70
Ambient temperature	Ta (C):	21.00

At elevation z, the plume has:

Centerline temperature	46	C	115	F
Virtual origin at	0.7	m	2.3	ft
Mean flame height of	9.4	m	30.9	ft

Example Output (English Units)

Steady Filling Equation (Solve for z)

Height of smoke layer during atrium filling from a steady fire

ceiling height above fire	H (ft):	98.40
cross-sectional area of atrium	A (ft^2):	53800.00
heat release rate of fire	Q (Btu/s):	4740.00
time	t (s):	200.00

Height of smoke layer above fire, z is 17.4 m or 57.2 ft

Steady Filling Equation (Solve for t)

Atrium filling time for steady fire

ceiling height above fire	H (ft):	131.00
cross-sectional area of atrium	A (ft^2):	107000.00
heat release rate of fire	Q (Btu/s):	4740.00
height of smoke layer above fire	z (ft):	26.20

Filling time is 1283 seconds or 21.4 min.

Unsteady Filling Equation (Solve for z)

Atrium filling time for unsteady fire

ceiling height above fire	H (ft):	98.40
cross-sectional area of atrium	A (ft^2):	86100.00
fire growth constant (Menu)	a (Btu/s^2):	0.04444
time	t (s):	800.00

At 800 seconds, the fire is 30006 kW or 28442 Btu/s.

Height of smoke layer above fire, z is 10.7 m or 35.0 ft

Example Output (English Units) Continued

Unsteady Filling Equation (Solve for t)

Atrium filling time for unsteady fire

ceiling height above fire	H (ft):	164.00
cross-sectional area of atrium	A (ft^2):	129000.00
fire growth constant (Menu)	a (Btu/s^2):	0.04444
height of smoke layer above fire	z (ft)	32.80

Filling time is 1236 seconds or 20.6 min.
At this time, the fire is 71650 kW or 67914 Btu/s.

Simple plume equation

mass flow and temperature rise of an plume

without correction for virtual origin

Elevation	z (ft):	164.00
Heat release rate of fire	Q (Btu/s):	23700.00
Ambient temperature	Ta (F):	70.00

At elevation z, the plume has:

Mass flow of	1281.9 kg/s	2826.2 lb/s
Volumetric flow of	1117.2 m^3/s	2367054 cfm
Average temperature of	35 C	94 F
Mean flame height of	8.3 m	27.1 ft

Example Output (English Units) Continued

Plume With Virtual Origin Correction

Mass flow rate and average plume temperature

Elevation	z	(ft):	164.00
Heat release rate of fire	Q	(Btu/s):	23700.00
fire diameter	Df	(ft):	13.10
Ambient temperature	Ta	(F):	70.00

At elevation z, the plume has:

Mass flow of	1253.9	kg/s	2764.4	lb/s
Volumetric flow of	1093.9	m^3/s	2317599	cfm
Average temperature of	35	C	95	F
Virtual origin at	0.7	m	2.3	ft
Mean flame height of	9.4	m	30.9	ft

Plume Centerline Temperature

calculate centerline plume temperature

Elevation	z	(ft):	164.00
Heat release rate of fire	Q	(Btu/s):	23700.00
fire diameter	Df	(ft):	13.10
Convective fraction of heat release	(0.6 to 1):		0.70
Ambient temperature	Ta	(F):	70.00

At elevation z, the plume has:

Centerline temperature	46	C	116 F
Virtual origin at	0.7	m	2.3 ft
Mean flame height of	9.4	m	30.9 ft

Appendix E ASET-C: A Room Fire Program for Personal Computers

1. INTRODUCTION

Cooper (1981) of the Center for Fire Research, National Bureau of Standards introduced ASET, a mathematical model for estimating Available Safe Egress Time in fires. Cooper and Stroup (1982) published a computer program to perform the calculations in the mathematical model, thus, the computer program also became known as ASET. ASET was not specifically written for the personal computer environment because at the time it was being developed, personal computers were just emerging as a tool for use in the engineering office.

Since the introduction of ASET, the use of personal computers has become widespread and there has been significant interest in running ASET on personal computers. In response to this interest, Walton (1985) introduced ASET-B, a program for personal computers based on the original ASET mathematical model. The B was used to indicate basic, brief, BASIC and Beta.

ASET is a 1500 line FORTRAN program that has many features. ASET-B is a 100 line BASIC program that was developed to be as simple and fast as possible. The most significant change in ASET-B is the use of a different mathematical procedure to solve the primary equations. ASET-B employs an equation solver that is at least 5 times faster than that used in ASET, while retaining mathematical agreement to within a fraction of a percent. ASET-B is an interactive program requiring a minimum of input. These features make ASET-B easy to learn and apply. In many conversations with practicing fire protection engineers, the author has found that ASET-B has become very popular.

This appendix describes the ASET-C routine which is part of the ASMET program. ASET-C is a C language version of ASET-B with improved interactive input and few added features. The interactive input was made to be consistent with the other ASMET routines. The added features consist of allowing fire data input from a file and the use of a t-square fire. Most of the material in this appendix is adapted from Walton's (1985) paper on ASET-B, and in many places the adaptation consisted of only changing ASET-B to ASET-C.

2. DESCRIPTION OF THE MODEL

The mathematical model which is the basis for ASET, ASET-B and ASET-C has been presented in detail by Cooper (1981, 1982), and will be only summarized here. It is based on a single room or enclosure with all doors, windows or vents closed except for a small leak at floor level. This leak prevents the pressure from increasing in the room. A fire starts at some point below the ceiling and releases energy and products of combustion. The rate at which energy and products of combustion are released may change with time. The hot products of combustion form a plume, which due to buoyancy, rises towards the ceiling. As the plume rises, it draws in cool air from the room which decreases the plume's temperature and increases its volume flow rate. When the plume reaches the ceiling it spreads out and forms a hot gas layer, which descends with time as the plume's gases continue to flow into it. There is

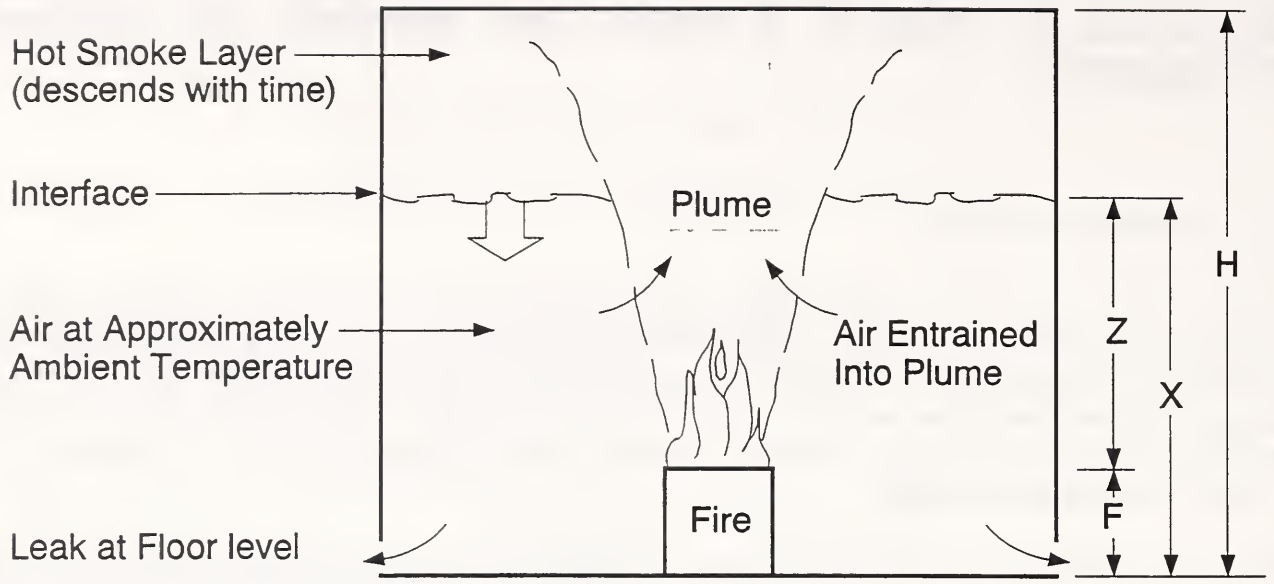

Figure E1. Schematic of fire phenomena

a relatively sharp interface between the hot upper layer and the air in the lower part of room, which in this model is considered to be at ambient temperature. The only interchange between the air in the lower part of the room and the hot upper layer is through the plume. ASET could therefore be described as a two layer or zone model. The basic fire phenomena are shown schematically in figure E1.

The two unknowns in ASET-C are the height of the hot layer interface above the fire, Z, and the average temperature of the upper layer, P. It should be noted that the notation used here to describe the model is consistent with the variable names used in the computer program. The unknowns, Z and P, are often referred to as the (dimensionless) height and temperature of the smoke layer since, consistent with the model formulation, smoke can only be found in the plume and the hot upper layer. The known quantities are the area and height of the room, A and H, the height of the base of the fire above the floor, F, and the acceleration due to gravity, G. In addition, the ambient temperature, PA, density, DA, and specific heat, CP, of air must be known. The final known quantities are the rate at which heat is released by the fire as a function of time, QT, the fraction of the total heat release which is given off as radiation, LR, and the fraction of total heat release rate which is lost to the contents and surrounding surfaces of the room, LC.

The unknown height and temperature are determined by using conservation of mass and energy in conjunction with equations describing the plume. Since the height and temperature of the smoke layer will vary with time, T, their solutions are obtained by solving two differential equations. In developing the original equations for ASET (Cooper 1981, 1982), two dimensionless groups of problem parameters, C1 and C2, were introduced. Also introduced were dimensionless forms of the variables time, height and temperature of the smoke layer, initial height of the smoke layer, height of the base of the fire and the rate of heat release. These variables are made dimensionless by dividing them by a characteristic quantity with the same dimensions or units. Thus the dimensionless temperature, P, is the actual temperature of the smoke layer, PF (converted to R), divided by the ambient temperature, PA (R). Similarly, the dimensionless rate of heat release, QT, is the actual rate of heat release, QA (kW), divided by the initial rate of heat release, Q0 (kW). Finally, the dimensionless variables, height of the smoke

layer, Z, initial height of the smoke layer, Z0, and height of the base of the fire, F, are the dimensional values for these variables in feet divided by a characteristic length CL which is also in feet. Here as in the ASET program, CL is simply taken as one foot. Thus the dimensionless lengths Z, Z0 and F are the same as their physical lengths in feet. The dimensionless time, T, is the actual time divided by a characteristic time, CT, of one second. The dimensionless time, T, is therefore numerically equal to the actual time in seconds. Since engineering units are used in ASET, this convention has been continued here for consistency. Conversion to SI units is provided in the computer program.

The differential equations for the dimensionless height of the layer above the fire, Z, and average temperature of the layer, P, are given below.

$$\frac{dZ}{dT} = \begin{cases} -C1\cdot QT - C2\cdot QT^{1/3}Z^{5/3} & \text{for } 0<Z<Z0 \\ -C1\cdot QT & \text{for } -F<Z\le 0 \\ 0 & \text{for } Z = -F \end{cases}$$

$$\frac{dP}{dT} = \begin{cases} P[C1\cdot QT - (P-1)C2\cdot QT^{1/3}Z^{5/3}]/(ZO+Z) & \text{for } 0<Z<Z0 \\ P\cdot C1\cdot QT/(Z0+Z) & \text{for } -F\le Z\le 0 \end{cases}$$

$$C1 = (1 - LC)\cdot QO\cdot CT/(DA\cdot CP\cdot PA\cdot A\cdot CL)$$
$$C2 = (0.21\cdot CT/A)[(1 - LR)\cdot QO\cdot G\cdot CL^2/(DA\cdot CP\cdot PA)]^{1/3}$$

In order to solve the equations for Z and P the initial conditions must be known. One set of initial conditions which were derived in (Cooper 1981, 1982), and will be used here, assume that the fire starts with a small heat release rate, Q0, at time T=0. Under such conditions the initial conditions are.

$$Z = ZO$$
$$P = 1 + Z0^{-5/3}C1/C2$$

Although dP/dT is indeterminate in the above equation at T=0 its actual value has been found in (Cooper 1981, 1982) to be.

$$\frac{dP}{dT} = \frac{C1}{C2}\,\frac{2\cdot DQO + (C1 + C2\cdot ZO^{5/3})}{6\cdot ZO^{8/3}}$$

where DQ0=dQT/dT at time T=0.

3. SOLUTION OF THE EQUATIONS

In general, the differential equations for Z and P cannot be solved explicitly, that is, an algebraic expression cannot be written which describes Z and P at any time T. As a result, the equations must be

solved numerically. ASET solves the differential equations using a variation of the fourth-order Runge-Kutta method with variable time step. While this method has a high degree of accuracy, it has been determined that the improved Euler's method has sufficient accuracy for this problem. The improved Euler's method is a simple predictor-corrector type and is described in most books on numerical methods (Carhanan, Luther, and Wilkes 1969). The improved Euler's method used in ASET-C requires substantially fewer calculations than the method used in ASET, resulting in ASET-C running much faster than ASET.

The improved Euler's method as applied in ASET-C is basically a technique for stepping the solution forward in time. Given the values of Z and P at a particular time, T, the method is used to determine the values of Z and P at time, T+DT, where DT is a small time increment. This process is started at time T=0 and continued until Z and P are known at all times of interest. In the case of ASET-C an increment of 1 second has been found to yield results which agree well with ASET for problems of practical interest.

In ASET-C, Z1 and P1, are used to indicate the values of Z and P at time, T. For the first step these are the initial values at time, T=0. Z2 and P2 are used to indicate the values of Z and P to be calculated at time, T+DT. To determine Z2 and P2 it is observed that the differential equations for Z and P represent the time rate of change of these quantities. The time rate of change multiplied by the time step yields the change which occurs over the time step. This would be an exact result if the equations were linear or the time steps were infinitely small. Since the equations are nonlinear, and it is impractical to make the time step infinitely small, an approximation must be used. In the improved Euler's method, Z2 and P2 are first predicted using the derivatives evaluated at time, T. Using Z2 and P2 the derivatives are then evaluated at time, T+DT. Corrected values of Z2 and P2 are then calculated using the average of the derivatives evaluated at times T, and, T+DT. Z2 and P2 are predicted by

$$Z2 = Z1 + DZ1 \cdot DT$$
$$P2 = P1 + DP1 \cdot DT$$

where DZ1=dZ/dT and DP1=dP/dT are evaluated using Z=Z1 and P=P1. The derivatives at time T+DT, DZ2=dZ/dT and DP2=dP/dT, are then evaluated using Z=Z2 and P=P2. Corrected values for Z2 and P2 are calculated using the average derivatives.

$$Z2C = Z1 + [(DZ1 + DZ2)/2] \cdot DT$$
$$P2C = P1 + [(DP1 + DP2)/2] \cdot DT$$

The predicted values of Z and P are then compared to the corrected values. In ASET-C if the absolute value of the difference between the predicted and corrected values is less than 0.001, the solution is considered to have converged and the program proceeds to the next time step. If the difference is greater than 0.001 the predicted values become the corrected values and the derivatives at time, T+DT, are recalculated. New corrected values are then calculated. In ASET-C this procedure is repeated for a maximum of thirty times. If the differences are still greater than 0.001, a warning is printed, and the program proceeds to the next time step.

The evaluation of the derivatives of Z and P requires the dimensionless heat release rate, QT, be known for all times, T. For heat release rates which are not constant with time, ASET-C requires the heat release be specified for each one second time interval. To simplify this procedure, ASET-C uses point specified heat release rates with linear interpolation. Heat release rates can be specified at as many as

100 different times. Linear interpolation is then performed to determine the heat release rate at each time step.

4. RUNNING THE PROGRAM

4.1 General Instructions

ASET-C is written as an interactive program, that is, the program prompts the user with questions. As previously stated, ASET-C is part of the ASMET package of routines for atrium analysis, and the general input instructions are provided in appendix D. The mechanics of input for ASET-C are consistent with the other routine in this package, and readers familiar with computer programs may not have to bother appendix D. To use ASET-C data must be entered for the items discussed below.

4.2 Program Inputs

4.2.1 Heat Loss Fraction

The second input is the heat loss fraction. This quantity is the instantaneous faction of the heat release rate of the fire which is lost to the bounding surfaces of the room and its contents. Cooper (1981, 1982) has provided guidelines for selecting this parameter which is called Lambda C or ALMAC in ASET. He has determined that the approximate range is 0.6 - 0.9. The lower value corresponds to high aspect ratio spaces (ratio of ceiling span to room height) with smooth ceilings and fires positioned far away from the walls. The intermediate to high values correspond to low aspect ratio spaces, rooms with irregular surfaces or rooms in which the fire is within one ceiling height of the wall. The temperature of the upper layer is a function of the heat loss fraction and the heat release rate of the fire. The greater the heat loss fraction the lower the temperature in the upper layer. The heat loss fraction for a room with insulated walls will be lower than the fraction for the same room with uninsulated walls.

Both ASET and ASET-C treat the heat loss parameter as a constant. That is, the heat lost from the room is a constant fraction of the heat release rate of the fire. As the heat release rate of the fire changes the quantity of heat lost will also change but in direct proportion to the fire. Therefore the room will not cool down even though the heat release rate of the fire goes to zero.

4.2.2 Height of the Base of the Fire

The third input is the height of the base of the fire above the floor in feet. For fuel items of relatively uniform surface height, such as beds, this is simply the height of the surface. For three dimensional fuel items, such as sofas, an average height weighted to reflect the distribution of surfaces should be used. The rate of growth of the upper layer is strongly dependent on the difference between the height of the base of the fire and the height of the smoke layer interface.

4.2.3 Room Ceiling Height and Floor Area

The fourth and fifth inputs are the room ceiling height in feet and the floor area in square feet. According to Cooper (1981, 1982) the calculations may not be valid when applied to room length-to-width aspect ratios greater than 10:1, or with a ratio of height to minimum horizontal dimension

exceeding one. The equations are based on the assumption that the upper layer is well mixed and at a uniform temperature. Therefore the results for a square room and a rectangular room of equal height and area will be the same.

4.2.4 Output Interval

The output interval is the time step for results that are sent to the screen or printed. The output interval of ASET-B was set at 5 seconds, and this is the default interval for ASET-C.

4.2.5 Maximum Time

The sixth input is the maximum time for the simulation in seconds. The results of the calculations will be printed at five second intervals until the maximum time or until the end of the heat release data.

4.2.6 Fire Growth Constant

The final input is the description of heat release rate of the fire. A fire growth constant can be entered to define a t-squared fire, or a menu can be activated that allows selection a fire growth constant for typical fires (slow, medium, fast or ultra-fast). Further the user can choose to enter data as sets of points as was done with ASET-B. When the user selects data points, the computer waits for the run command to request the data. However, the following is a discussion of input by data points.

As described earlier the program can accommodate up to 100 pairs of times and corresponding heat release rates. The program performs a linear interpolation between the specified points to determine the heat release rates at the required times during the calculations. The data is entered by typing the time in seconds, followed by a comma, followed by the heat release rate in kilowatts. A return or enter is then typed to proceed to the next line.

Heat release rates entered as less than 0.1 kilowatts will be converted to that value. The program will automatically assume a starting value 0.1 kilowatts at time zero. A heat release rate at time zero does not have to be entered unless a greater initial heat release rate is required. When all of the desired times and heat release rates have been entered a -9,-9 followed by a return is entered to terminate the data entry and begin the calculations. Actually any negative time followed by a heat release rate will result in the same action.

4.2.7 Optional Upper Limit on Fire

Fire growth may be approximated by the t-squared curve for some time. Because of the action of a suppression system, limitations of fuel, or limitations of combustion air; t-squared fire growth eventually must stop. The optional upper limit on fire growth allows the user to specify a heat release rate at which the fire curve reaches steady burning.

4.2.8 Send Results to Printer or to File

To sent results to the printer, press **P**. To send results to a file, press **t** and enter the file name.

4.2.8 Run Simulation

To run ASET-C, press **R**. If data heat release rate by point entry has been selected. The data points will be requested after the run starts.

4.3 Program Outputs

The output of the ASET-B program is a summary of the input data and a table of the conditions in the room as a function of time. The first column in the table is the simulation time in seconds. The second and third columns are the temperature in the upper layer in degrees Celsius and Fahrenheit. The fourth and fifth columns are the height above the floor of the interface between the upper and lower layers. The sixth and seventh columns are the heat release rate of the fire in kilowatts and BTU per second. The output has the same number of significant digits as does ASET-B, which allows users to verify that this program produces the same results as ASET-B for the same input.

5. LIMITATIONS OF THE ASET

The use of ASET-C or any design aid requires the design engineer to make the final evaluation as to the appropriateness of the design. The ASET-C programs are based on certain engineering approximations of the fire environment and should be used to supplement rather than replace sound engineering judgement. The program results should be treated as approximate and the user is encouraged to become familiar with how changes in the input variables effect the program results. The temperature of the upper layer and the height of the interface respond differently to changes in the input data. Appropriate factors of safety should be applied to either the input data or the program results.

Some of the limitations of the program have been presented in conjunction with the input data requirements. There are however, some additional limitations. The mathematical procedure used in ASET-C is very hardy, that is, the procedure will normally converge and produce results. There are combinations of input data for which the program will either fail to converge or halt due to an illegal mathematical operation. If the procedure for solving the equations fails to converge, a warning will be printed and the solution will continue. The results following this message may be in error and should be treated as such. The failure to converge is usually a result of a heat release value which changes too rapidly. In most cases this problem can be corrected by minor smoothing of the input heat release curve.

6. VERIFICATION OF ASET

Results of the ASET program have been compared to data from a limited number of actual fire experiments (Cooper 1981, 1982). These comparisons can be extended to the ASET-B and ASET-C programs since they produce results which are within a few percent of those produced by ASET. The fire experiments considered a mockup of a hospital room-corridor building space. Comparisons were found to be generally favorable. This does not necessarily mean that the comparison will be favorable in all cases. Clearly additional studies are required in this area and that work is ongoing.

7. SAMPLE RUN (SI Units)

```
HEAT LOSS FRACTION =     0.80
FIRE HEIGHT =     0.00 m
ROOM HEIGHT =     3.00 m
ROOM AREA   =    20.00 sq m
fire growth constant (kW/s^2 ): 0.046890
```

TIME sec	TEMP C	TEMP F	LAYER m	LAYER ft	FIRE kW	FIRE Btu/s
0.0	21.2	70.2	3.0	9.8	0.1	0.1
5.0	21.5	70.6	2.9	9.6	1.2	1.1
10.0	21.9	71.5	2.8	9.2	4.7	4.4
15.0	22.6	72.6	2.7	8.8	10.6	10.0
20.0	23.3	74.0	2.5	8.2	18.8	17.8
25.0	24.3	75.7	2.3	7.6	29.3	27.8
30.0	25.4	77.8	2.2	7.1	42.2	40.0
35.0	26.8	80.2	2.0	6.5	57.4	54.5
40.0	28.4	83.1	1.8	5.9	75.0	71.2
45.0	30.3	86.6	1.6	5.4	95.0	90.1
50.0	32.5	90.5	1.5	4.9	117.2	111.2
55.0	35.1	95.2	1.3	4.4	141.8	134.5
60.0	38.1	100.5	1.2	4.0	168.8	160.1
65.0	41.5	106.6	1.1	3.6	198.1	187.9
70.0	45.3	113.6	1.0	3.2	229.8	217.9
75.0	49.8	121.6	0.9	2.8	263.8	250.2
80.0	54.8	130.6	0.8	2.5	300.1	284.6
85.0	60.5	140.8	0.7	2.2	338.8	321.3
90.0	66.9	152.4	0.6	1.8	379.8	360.2
95.0	74.1	165.3	0.5	1.5	423.2	401.4
100.0	82.1	179.9	0.4	1.2	468.9	444.8
105.0	91.2	196.1	0.3	1.0	517.0	490.3
110.0	101.3	214.3	0.2	0.7	567.4	538.1
115.0	112.5	234.4	0.1	0.4	620.1	588.2
120.0	124.8	256.7	0.0	0.1	675.2	640.4
125.0	138.5	281.3	0.0	0.0	732.7	694.9
130.0	153.8	308.8	0.0	0.0	792.4	751.6
135.0	171.0	339.8	0.0	0.0	854.6	810.6
140.0	190.3	374.5	0.0	0.0	919.0	871.7
145.0	211.9	413.4	0.0	0.0	985.9	935.1
150.0	236.2	457.1	0.0	0.0	1055.0	1000.7
155.0	263.5	506.3	0.0	0.0	1126.5	1068.5
160.0	294.3	561.7	0.0	0.0	1200.4	1138.6
165.0	329.0	624.1	0.0	0.0	1276.6	1210.8
170.0	368.1	694.6	0.0	0.0	1355.1	1285.3
175.0	412.5	774.4	0.0	0.0	1436.0	1362.1
180.0	462.7	864.9	0.0	0.0	1519.2	1441.0

8. SAMPLE RUN (English Units)

```
HEAT LOSS FRACTION =     0.80
FIRE HEIGHT =     1.00 ft
ROOM HEIGHT =     9.00 ft
ROOM AREA   =   225.00 sq ft

Fire curve input manually
 TIME (sec), HEAT RELEASE RATE (kW):       20,      400
 TIME (sec), HEAT RELEASE RATE (kW):      100,     2000
```

```
TIME (sec), HEAT RELEASE RATE (kW):      180,     5000
TIME (sec), HEAT RELEASE RATE (kW):       -9,       -9
```

TIME sec	TEMP C	TEMP F	LAYER m	LAYER ft	FIRE kW	FIRE Btu/s
0.0	21.3	70.3	2.7	9.0	0.1	0.1
5.0	23.4	74.2	2.7	8.7	10.1	9.6
10.0	24.9	76.7	2.5	8.3	20.1	19.0
15.0	26.3	79.3	2.4	7.8	30.0	28.5
20.0	27.7	81.8	2.2	7.3	40.0	37.9
25.0	29.2	84.6	2.1	6.9	50.0	47.4
30.0	30.8	87.5	2.0	6.5	60.0	56.9
35.0	32.6	90.6	1.8	6.0	70.0	66.4
40.0	34.4	93.9	1.7	5.7	80.0	75.9
45.0	36.4	97.5	1.6	5.3	90.0	85.4
50.0	38.6	101.4	1.5	5.0	100.0	94.8
55.0	40.9	105.6	1.4	4.7	110.0	104.3
60.0	43.3	110.0	1.3	4.4	120.0	113.8
65.0	46.0	114.7	1.2	4.1	130.0	123.3
70.0	48.8	119.8	1.2	3.9	140.0	132.8
75.0	51.8	125.2	1.1	3.6	150.0	142.3
80.0	55.0	130.9	1.0	3.4	160.0	151.8
85.0	58.3	137.0	1.0	3.2	170.0	161.2
90.0	61.9	143.5	0.9	3.0	180.0	170.7
95.0	65.8	150.4	0.9	2.8	190.0	180.2
100.0	69.8	157.6	0.8	2.6	200.0	189.7
105.0	74.2	165.5	0.8	2.5	218.8	207.5
110.0	79.0	174.2	0.7	2.3	237.5	225.3
115.0	84.3	183.7	0.7	2.1	256.2	243.1
120.0	90.0	194.0	0.6	2.0	275.0	260.8
125.0	96.2	205.1	0.6	1.8	293.8	278.6
130.0	102.9	217.2	0.5	1.7	312.5	296.4
135.0	110.1	230.1	0.5	1.5	331.2	314.2
140.0	117.7	243.9	0.4	1.3	350.0	332.0
145.0	125.9	258.7	0.4	1.2	368.8	349.8
150.0	134.6	274.3	0.3	1.0	387.5	367.5
155.0	143.7	290.7	0.2	0.8	406.2	385.3
160.0	153.3	307.9	0.2	0.6	425.0	403.1
165.0	163.3	325.9	0.1	0.4	443.8	420.9
170.0	173.7	344.6	0.1	0.2	462.5	438.7
175.0	184.5	364.2	0.0	0.0	481.2	456.5
180.0	195.9	384.7	0.0	0.0	500.0	474.2

9. REFERENCES

Carhanan, B.; Luther, H.A.; Wilkes, J.O. 1969. Applied Numerical Methods. New York: John Wiley & Sons.

Cooper, L.Y. 1981. Estimating Safe Available Egress Time from Fires. Nat. Bur. Stand. (U.S.) NBSIR 80-2172.

Cooper, L.Y. 1982. A Mathematical Model for Estimating Available Safe Egress Time in Fires. Fire Mater. 6(3/4).

Cooper, L.Y., Stroup, D.W. 1982. Calculating Safe Egress Time (ASET) - A Computer Program and User's Guide. Nat. Bur. Stand. (U.S.) NBSIR 82-2578.

Walton, W.D. 1985. ASET-B: A Room Fire Program for Personal Computers, National Bureau of Standards, NBSIR 85-3144-1.

Appendix F Physical Modeling

One option when the above methods are inappropriate, is fire testing in a reduced scale model, and there is considerable experience with application of physical models to fire technology. Many approaches can be taken to the physical modeling of smoke transport due to fires including Froude modeling, pressure modeling and analog modeling. Froude modeling preserves the Froude number. Pressure modeling is done in a pressure vessel to preserve both the Froude and Reynolds numbers. Analog modeling uses different fluids to simulate the buoyancy effects of hot gases (for example salt water with fresh water).

The approach recognized by NFPA 92B for atrium analysis is Froude modeling. Accordingly, this section reviews the foundations of Froude modeling with the intent of providing insight into the capabilities and limitations of this technique. Quintiere (1989) presents a general theoretical basis for physical modeling with a variety of fire applications, and the treatment of dimensionless constants presented later in this paper draws heavily upon the work of Quintiere. For further information about fire applications of physical modeling, readers are referred to Heskestad (1972, 1975), Williams (1969), and Hottel (1961). Dillon (1994) presents an application of Froude modeling to atrium smoke management.

1. Development of Dimensionless Groups

For the development of the dimensionless groups of interest, the governing equations of fluid dynamics that are listed below are in a one-dimensional form.

Conservation of Mass:

$$\frac{\partial \rho}{\partial t} + \frac{\partial (\rho u)}{\partial x} = 0 \tag{F1}$$

Conservation of momentum in vertical direction:

$$\rho\left(\frac{\partial u}{\partial t} + u\frac{\partial u}{\partial x}\right) = -\frac{\partial p'}{\partial x} + g(\rho_o - \rho) + \frac{4}{3}\mu\frac{\partial^2 u}{\partial x^2} \tag{F2}$$

where

$$p' = p - p_o \tag{F3}$$

and

$$\frac{dp_o}{dx} = -\rho_o g \tag{F4}$$

p_o is the ambient pressure distribution

Conservation of energy:

$$\rho C_p\left(\frac{\partial T}{\partial t} + u\frac{\partial T}{\partial x}\right) = k\frac{\partial^2 T}{\partial x^2} - 4\kappa\sigma T^4 + \int_0^{4\pi} \kappa I \, d\omega + \dot{Q}''' + \frac{\partial p}{\partial t} \tag{F5}$$

The equation of state is the perfect gas law already discussed:

$$p = \rho R T \tag{F6}$$

Dimensionless variables are defined below

$$\hat{x} = \frac{x}{l}$$

$$\hat{u} = \frac{u}{V}$$

$$\hat{p} = \frac{p}{p_*}$$

$$\hat{p}' = \frac{p'}{p_*}$$

$$\hat{\rho} = \frac{\rho}{\rho_o}$$

$$\hat{T} = \frac{T}{T_o}$$

$$\hat{t} = \frac{t}{\tau}$$

$$\hat{Q} = \frac{Q''' l}{\rho_o V C_p T_o}$$

$$\hat{I} = \frac{I}{\sigma T_o^4}$$

where

l = geometric length scale;
V = characteristic velocity;
τ = characteristic time;
T_o = ambient temperature;
p_o = ambient pressure;
ρ_o = ambient density;
p_* = characteristic pressure defect ($p_* = \rho V^2$).

By substituting the dimensionless variables into the governing equations and rearranging, the following nondimensional form of the governing equations can be developed.

Mass:

$$\pi_1 \frac{\partial \hat{\rho}}{\partial \hat{t}} + \frac{\partial (\hat{\rho}\,\hat{u})}{\partial \hat{x}} = 0 \tag{F7}$$

Momentum:

$$\hat{\rho}\left(\pi_1 \frac{\partial \hat{u}}{\partial \hat{t}} + \hat{u}\frac{\partial \hat{u}}{\partial \hat{x}}\right) = -\pi_2 \frac{\partial \hat{p}'}{\partial \hat{x}} + \pi_3(1 - \hat{\rho}) + \frac{4}{3}\pi_4 \frac{\partial^2 \hat{u}}{\partial \hat{x}^2} \tag{F8}$$

Energy:

$$\hat{\rho}\left(\pi_1 \frac{\partial \hat{T}}{\partial \hat{t}} + \hat{u}\frac{\partial \hat{T}}{\partial \hat{x}}\right) = \pi_3 \pi_5 \frac{\partial^2 \hat{T}}{\partial \hat{x}^2} + \left(\frac{\pi_6 \pi_7}{\pi_3 \pi_5}\right)\left(\int_0^{4\pi} \hat{I}\,d\omega - 4\hat{T}^4\right) + \hat{Q} + \pi_8 \frac{\partial \hat{p}}{\partial \hat{t}} \tag{F9}$$

State:

$$\hat{p} = \left(\frac{1 - \pi_9}{\pi_8}\right)\hat{\rho}\,\hat{T} \tag{F10}$$

The dimensionless groups from the above equations are:

$$\begin{aligned}
\pi_1 &= \frac{l}{V\tau} = 1, \quad \tau = \frac{l}{V} \\
\pi_2 &= \frac{p_*}{\rho_o V^2} = 1, \quad p_* = \rho_o V^2 \\
\pi_3 &= \frac{gl}{V^2} = \frac{1}{Fr} \quad \text{where } Fr \text{ is the Froude number} \\
\pi_4 &= \frac{\mu}{\rho_o V l} = \frac{1}{Re} \quad \text{where } Re \text{ is the Reynolds number} \\
\pi_5 &= \frac{k}{\mu C_p} = \frac{1}{Pr} \quad \text{where } Pr \text{ is the Prandtl number} \\
\pi_6 &= \kappa l \\
\pi_7 &= \frac{\sigma T_o^3 l}{k} \\
\pi_8 &= \frac{l p_*}{\rho_o C_p V T_o \tau} = \frac{V^2}{C_p T_o} \quad \text{(by substitution of } \pi_1 \text{ and } \pi_2\text{)} \\
\pi_9 &= \frac{C_v}{C_p}
\end{aligned} \tag{F11}$$

2. Froude Modeling

In Froude modeling, a model of the atrium or other room is built, such that every dimension is an exact fraction of the full scale facility. Tests are conducted in the model in air at normal atmospheric conditions. Temperatures from the model are the same for corresponding places in the full scale facility.

The concept of similarity in physical modeling is that the important dimensionless groups be the same for corresponding locations in the model and the full scale facility. The Froude number can be thought of as the ratio of inertia forces to gravity forces. Because buoyancy is a gravity force and dominates the flow resulting from fires, the Froude number must be preserved. Because the tests are in air, groups π_5 and π_9 are also preserved. Because viscous effects at surfaces are not considered essential, the Reynolds number is ignored. It is not possible to preserve all of the heat transfer groups (π_6, π_7, π_8).

The scaling relation for temperature is:

$$T_m = T_f \tag{F12}$$

where
T_m = temperature of gas in model, °C (°F);
T_f = temperature of gas in full scale facility, °C (°F).

As stated above, this means that the temperatures from the model are the same for corresponding places in the full scale facility.

The scaling relation for density is:

$$\rho_m = \rho_f \tag{F13}$$

where
ρ_m = density of gas in model, kg/m^3 (lb/ft^3);
ρ_f = density of gas in full scale facility, kg/m^3 (lb/ft^3).

Preservation of the Froude number can be expressed as

$$\mathrm{Fr} = \frac{V_m^2}{g\, l_m} = \frac{V_f^2}{g\, l_f} \tag{F14}$$

where
V_m = velocity in the model, m/s (ft/s);
V_f = velocity in the full scale facility, m/s (ft/s);
l_m = length in the model, m (ft);
l_f = length in the full scale facility, m (ft);
g = acceleration of gravity, m/s^2 (ft/s^2).

The scaling relationship for velocity follows

Volumetric flow is velocity multiplied by area, the relation becomes

$$V_m = V_f \sqrt{\frac{l_m}{l_f}} \tag{F15}$$

$$\dot{V}_m = \dot{V}_f \left(\frac{l_m}{l_f}\right)^{5/2} \tag{F16}$$

where

$\dot{V}_m$ = volumetric flow in model, m^3/s (ft^3/s);

$\dot{V}_f$ = volumetric flow in full scale facility, m^3/s (ft^3/s).

Mass flow rate is volumetric flow multiplied by density, so combining equations (F13) and (F16) results in

$$\dot{m}_m = \dot{m}_f \left(\frac{l_m}{l_f}\right)^{5/2} \tag{F17}$$

where

$\dot{m}_m$ = mass flow in model, kg/s (lb/s);

$\dot{m}_f$ = mass flow in full scale facility, kg/s (lb/s).

Velocity is length per unit time, and substituting $V_m = l_m/t_m$ and $V_f = l_f/t_f$ into equation (F14) results in

$$t_m = t_f \sqrt{\frac{l_m}{l_f}} \tag{F18}$$

where

t_m = time in model, s;

t_f = time in full scale facility, s.

Consider the heat convective portion of the heat release rate as enthalpy flows, $Q_m = \dot{m}_m C_p \Delta T$ and $Q_f = \dot{m}_f C_p \Delta T$ ($\Delta T = \Delta T_m = \Delta T_f$), then equation (F17) becomes

$$Q_m = Q_f \left(\frac{l_m}{l_f}\right)^{5/2} \tag{F19}$$

where

Q_m = heat release rate in model, kW (Btu/s);

Q_f = heat release rate in full scale facility, kW (Btu/s).

Velocity pressure is $p_m = \rho V_m^2/2$ and $p_m = \rho V_m^2/2$, and substituting this into equation (F14) yields

$$p_m = p_f\left(\frac{l_m}{l_f}\right) \tag{F20}$$

where

p_m = pressure in model, Pa (in H_2O);
p_f = pressure in full scale facility, Pa (in H_2O).

Even though Reynolds number was explicitly ignored in the above analysis, some surface effects can be partially preserved by considering surface heat transfer and solid heat transfer. For a semi-infinite surface, the wall and ceiling materials can be scaled by

$$(k\,\rho\,c)_{w,m} = (k\,\rho\,c)_{w,f}\left(\frac{l_m}{l_f}\right)^{.9} \tag{F21}$$

where

$(k\rho c)_{w,m}$ = $k\rho c$ of the wall or ceiling material of the model, $kW^2\ m^{-4}\ K^{-2}s$ (Btu^2 in $h^{-1}\ ft^{-5}\ °F^{-2}$);
$(k\rho c)_{w,f}$ = $k\rho c$ of the wall or ceiling material of the full scale facility, $kW^2\ m^{-4}\ K^{-2}s$ (Btu^2 in $h^{-1}\ ft^{-5}\ °F^{-2}$).

The term $k\rho c$ is the product of the thermal conductivity, the density and the specific heat, and values of $k\rho c$ for several materials are listed in table F1.

It is important that the scale of the model be selected so that flow in the model has the turbulent characteristics of that in the full scale facility. For modeling smoke movement away from the fire and not plume development, the smallest length that can support such turbulent flow is often taken as about 0.3 m (1 ft). The following example illustrates the selection of the scale for a model. Consider that it is desired to realistically determine flows in openings from the atrium to the communicating spaces, these openings are 2.4 m (8 ft) high. These openings should not be less than about 0.3 m (1 ft) in the model. Thus the model should be 1/8 scale. The scale for each modelling application should be determined by consideration of what flows are important to simulate.

There has been considerable experience with Froude modeling, and the comparison between full scale and 1/7 scale model temperatures (figure F1) by Quintiere, McCaffrey and Kashiwagi (1978) illustrates the degree of agreement that can be expected.

3. References

Dillon, M.E. 1994. Determining Effectiveness of Atria Smoke Control Systems, ASHRAE Journal, Vol 36, No 4, pp 37-41.

Heskestad, G. 1972. Similarity Relations for the Initial Convective Flow Generated by Fire, Paper 72-WA/HT-17, American Society of Mechanical Engineers.

Heskestad, G. 1975. Physical Modeling of Fire, J. Fire & Flammability, Vol 6, pp 253-272.

Hottel, H.C. 1961. Fire Modeling. The Use of Models in Fire Research, Publication 786 National Academy of Sciences, Washington DC, pp 32-47.

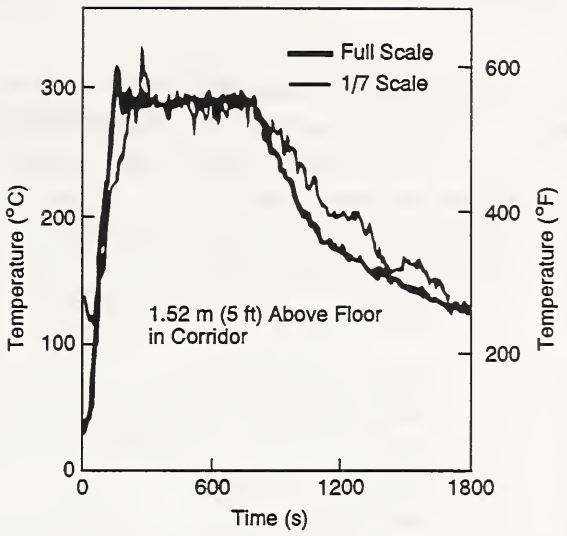

Figure F1. Froude modeling comparison of corridor gas temperature

Quintiere, J.G. 1989. Scaling Applications in Fire Research, Fire Safety Journal, Vol 15, No 1, pp 3-29.

Quintiere, J.G., McCaffrey, B.J. and Kashiwagi, T. 1978. Combustion Science and Technology, Vol 18, pp 1-19.

Williams, F.A. 1969. Journal of Fire and Flammability, Vol 6, pp 253-273.

4. Nomenclature

g = acceleration of gravity
k = thermal conductivity
$(k\rho c)_{w,f}$ = $k\rho c$ of the wall or ceiling material of the full scale facility
$(k\rho c)_{w,m}$ = $k\rho c$ of the wall or ceiling material of the model
l = geometric length scale
l_f = length in the full scale facility
l_m = length in the model
$\dot{m}_f$ = mass flow in full scale facility
$\dot{m}_m$ = mass flow in model
p_* = characteristic pressure defect ($p_* = \rho V^2$)
p_f = pressure in full scale facility
p_m = pressure in model
p_o = ambient pressure
Q_f = heat release rate in full scale facility
Q_m = heat release rate in model
t_f = time in full scale facility
T_f = temperature of gas in full scale facility
t_m = time in model
T_m = temperature of gas in model
T_o = ambient temperature
V = characteristic velocity
V_f = velocity in the full scale facility
V_m = velocity in the model
$\dot{V}_f$ = volumetric flow in full scale facility
$\dot{V}_m$ = volumetric flow in model
ρ_f = density of gas in full scale facility
ρ_m = density of gas in model
ρ_o = ambient density
τ = characteristic time

Table F1. Thermal properties of materials [Adapted from McCaffrey, Quintiere, Harkleroad (1981)]

Material	Density ρ (kg/m^3)	Specific Heat c (kJ/kg K)	Thermal Conductivity k x 10^3 (kW/m K)	kρc $kW^2\ m^{-4}\ K^{-2}s$
Aluminum (pure)	2710	0.895	206	500
Concrete	2400	0.75	1.6	2.9
Asbestos-Cement Board (heavy)	2100	1.0	1.1	2.3
Brick	2600	0.8	0.8	1.7
Brick/Concrete Block	1900	0.84	0.73	1.2
Gypsum Board	960	1.1	0.17	0.18
Plasterboard	950	0.84	0.16	0.13
Plywood	540	2.5	0.12	0.16
Chipboard	800	1.25	0.15	0.15
Aerated Concrete	500	0.96	0.26	0.13
Cement-Asbestos Board	658	1.06	0.14	0.098
Calcium Silicate Board (Marinite XL)*	700	1.12	0.11-0.14	0.086-.11
Fiber Insulation Board	240	1.25	0.53	0.015
Alumina Silicate Block (Kaowool)*	260	~1	0.14	0.036
Glass Fiber Insulation	60	0.8	0.037	0.0018
Expanded Polystyrene	20	1.5	0.034	0.0010

Notes:

1. *Trade name - implies no endorsement by NIST.
2. Unit conversions: 1 kg/m^3 = 0.0624 lb/ft^3, 1 kJ/kg K = 2.39×10^{-4} Btu/lb°F; 1 kW/m K = 6.93 Btu in $hr^{-1}\ ft^{-5}\ °F^{-2}$; 1 $kW^2\ m^{-4}\ K^{-2}s$ = 1.03×10^{-4} Btu^2 in $h^{-1}\ ft^{-5}\ °F^{-2}$.

Appendix G Computational Fluid Dynamics

Computational fluid dynamics (CFD) consists of dividing a space into a large number of spaces, and obtaining approximate solutions to the fundamental equations of fluid dynamics for each space. CFD is sometimes called field modeling. Many computer CFD programs has been developed that are capable of simulation of fire induced flows. Friedman (1992) discusses ten such codes. Several of these are general purpose codes that are commercially available. The development of computer work stations that are capable of running meaningful simulations has lead to an increased use of CFD in many areas of engineering, and fire protection is no exception.

This appendix is an outline of the topic with the intent of providing some understanding of the capabilities and limitations of CFD with respect to smoke flow in atria. Because this appendix is intended for practicing engineers, it was written so that readers need only some knowledge of undergraduate fluid dynamics. The equations in this appendix are intended to describe CFD modeling and not be used for calculations. Accordingly, units are not given for variables of this section. However, all of these equations are valid for SI units or any other dimensionlly homogeneous unit system (see Appendix B).

Readers should be aware that a thorough knowledge of CFD requires extensive understanding of graduate level fluid dynamics. For more information on this topic readers are referred to Anderson, Tannehill and Pletcher (1984), Abbott and Basco (1989), Hoffmann (1989), Hirsch (1988; 1990), Kumar (1983), and Markatos (1986).

1. Fundamental Equations

This section lists the fundamental equations of fluid dynamics with the intent of giving readers an appreciation of the level of complexity of this topic. However, it is not expected that readers would have a significant understanding these equations without study of fluid dynamics at the graduate level.
In Cartesian coordinates, the velocity vector is expressed as

$$\boldsymbol{q} = \boldsymbol{i}u + \boldsymbol{j}v + \boldsymbol{k}w \tag{G1}$$

where u, v and w are velocity components in the x, y and z directions respectively. For unsteady, compressible, viscous flow; the conservation equations are written below.
Mass:

$$\frac{D\rho}{Dt} + \rho\nabla\cdot\boldsymbol{q} = 0 \tag{G2}$$

Momentum:

$$\rho\frac{Du}{Dt} = \rho X_x - \frac{\partial p}{\partial x} + \frac{\partial}{\partial x}\left[\mu\left(2\frac{\partial u}{\partial x} - \frac{2}{3}\nabla\cdot\boldsymbol{q}\right)\right] + \frac{\partial}{\partial y}\left[\mu\left(\frac{\partial u}{\partial y} + \frac{\partial v}{\partial x}\right)\right] + \frac{\partial}{\partial z}\left[\mu\left(\frac{\partial w}{\partial x} + \frac{\partial u}{\partial z}\right)\right] \tag{G3}$$

$$\rho\frac{Dv}{Dt} = \rho X_y - \frac{\partial p}{\partial y} + \frac{\partial}{\partial y}\left[\mu\left(2\frac{\partial v}{\partial y} - \frac{2}{3}\nabla\cdot\boldsymbol{q}\right)\right] + \frac{\partial}{\partial z}\left[\mu\left(\frac{\partial v}{\partial z} + \frac{\partial w}{\partial y}\right)\right] + \frac{\partial}{\partial x}\left[\mu\left(\frac{\partial u}{\partial y} + \frac{\partial v}{\partial x}\right)\right] \tag{G4}$$

$$\rho\frac{Dw}{Dt} = \rho X_z - \frac{\partial p}{\partial z} + \frac{\partial}{\partial z}\left[\mu\left(2\frac{\partial w}{\partial z} - \frac{2}{3}\nabla\cdot\boldsymbol{q}\right)\right] + \frac{\partial}{\partial x}\left[\mu\left(\frac{\partial w}{\partial x} + \frac{\partial u}{\partial z}\right)\right] + \frac{\partial}{\partial y}\left[\mu\left(\frac{\partial v}{\partial z} + \frac{\partial w}{\partial y}\right)\right] \tag{G5}$$

Energy:

$$\frac{\partial}{\partial x}\left(k\frac{\partial T}{\partial x}\right) + \frac{\partial}{\partial y}\left(k\frac{\partial T}{\partial y}\right) + \frac{\partial}{\partial z}\left(k\frac{\partial T}{\partial z}\right) + \Phi = \rho\frac{\partial(C_pT)}{\partial t} + \rho u\frac{\partial(C_pT)}{\partial x} + \rho v\frac{\partial(C_pT)}{\partial y} + \rho w\frac{\partial(C_pT)}{\partial z} - \left(\frac{\partial p}{\partial t} + u\frac{\partial p}{\partial x} + v\frac{\partial p}{\partial y} + w\frac{\partial p}{\partial z}\right) \tag{G6}$$

The dissipation function, Φ, represents the time rate at which energy is dissipated per unit volume through the action of viscosity, and this function can be expressed as

$$\Phi = -\frac{2}{3}\mu(\nabla\cdot\boldsymbol{q})^2 + 2\mu\left[\left(\frac{\partial u}{\partial x}\right)^2 + \left(\frac{\partial v}{\partial y}\right)^2 + \left(\frac{\partial w}{\partial z}\right)^2\right] + \mu\left[\left(\frac{\partial u}{\partial y} + \frac{\partial v}{\partial x}\right)^2 + \left(\frac{\partial v}{\partial z} + \frac{\partial w}{\partial y}\right)^2 + \left(\frac{\partial w}{\partial x} + \frac{\partial u}{\partial z}\right)^2\right] \tag{G7}$$

The symbol ∇ is called the gradient, and it is written as:

$$\nabla = \boldsymbol{i}\frac{\partial}{\partial x} + \boldsymbol{j}\frac{\partial}{\partial y} + \boldsymbol{k}\frac{\partial}{\partial z} \tag{G8}$$

The material derivative is defined as:

$$\frac{D}{Dt} = \frac{\partial}{\partial t} + \boldsymbol{q}\cdot\nabla = \frac{\partial}{\partial t} + u\frac{\partial}{\partial x} + v\frac{\partial}{\partial y} + w\frac{\partial}{\partial z} \tag{G9}$$

Equation of State:

In addition to the conservation equations, an equation relating pressure, temperature and density is needed. Such equations are called *equations of state*. The perfect gas law is frequently used in CFD applications:

$$p = \rho RT \tag{G10}$$

where R is the gas constant.

The conservation of momentum equations are often called the Navier-Stokes (N-S) equations, but the term N-S equations is also used in a broader sense to mean all the conservation equations plus the equation of state, and this paper the broader meaning is used. It is not possible here to discuss al of the assumptions involved in the derivation of N-S equations. However, two of the more important ones are the continuum assumption and the stress-strain relationship for a Newtonian fluid. For an exhaustive derivation of the N-S equations readers are referred to Aris (1962).

At the level of generality presented above, it is beyond the state of technology to solve the N-S equations exactly. Even with the simplifying assumptions of incompressibility or of Boussinesq[1] flow, it is still not possible to solve the three dimensional N-S equations exactly. Exact solutions have been obtained for a laminar flow in simple geometries, and the most notable application of inexact solutions are to boundary layer flows. Exact and inexact solutions are discussed in several texts (White 1974; Sherman 1990; Schlichting 1960; Schetz 1993). By experimental verification of these solutions, the N-S equations have themselves been verified for laminar flow. There is no such verification for turbulent flow. However, CDF simulations of turbulent flow based on the N-S equations as discussed below often corresponds well with experimental data.

2. Turbulence Modeling

Most CFD models use an approach called *large eddy simulation* which uses the N-S equation to simulate the evolution of large eddies and models the effects of the small eddies. Before modeling of small eddies is discussed, it should be mentioned that large eddy simulation is based on the conversion of the N-S equations to an averaged form of equations. All of the parameters in the governing equations are separated into average and fluctuating components. An assumption of this approach is that these fluctuations are random.

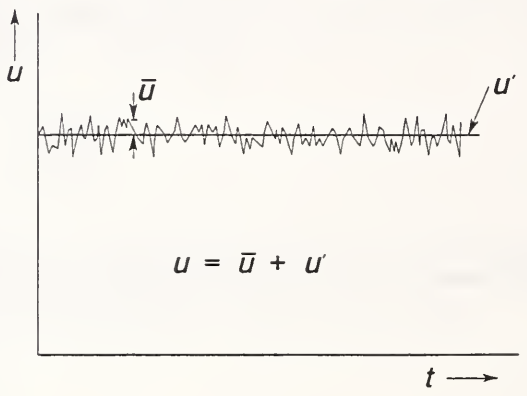

Figure G1. Time averaging approach of Reynolds

The quantity, $\bar{f}$, averaged over time, Δt, is defined as

$$\bar{f} = \frac{1}{\Delta t} \int_{t}^{t+\Delta t} f \, dt \qquad \text{(G11)}$$

The quantity, f, can be separated into averaged, $\bar{f}$, and fluctuating, f', components ($f = \bar{f} + f'$). Separation of u is illustrated in figure G1. In Reynolds decomposition, the fluctuating terms of the N-S equations become

[1]Boussinesq flow is an approximation to compressible flow that extends the incompressible flow equations by considering density as a function of temperature (Sherman 1990 p 84).

$$u = \bar{u} + u'; \quad v = \bar{v} + v'; \quad w = \bar{w} + w';$$
$$\rho = \bar{\rho} + \rho'; \quad p = \bar{p} + p'; \quad T = \bar{T} + T'. \tag{G12}$$

Substituting these into the N-S equations results in the Reynolds averaged N-S equations with additional terms that are related to the averaged flow variables by *turbulence models*. These turbulence models approximate the effect of the small eddies, and some of the common ones are the Prandtl algebraic model, the k-ε model and the Reynolds stress model.

Because the k-ε model is extensively implemented in CFD codes, a few details of it are given. This model was developed by analogy to incompressible boundary layer flow (Harlow and Nakayama 1968; Launder and Spalding 1974), and it consists of adding two partial differential equations to the averaged N-S equations. The term k is the kinetic energy of turbulence, and it is

$$k = \frac{1}{2}\overline{u_i' u_i'} = \frac{1}{2}\overline{(u'^2 + v'^2 + w'^2)} \tag{G13}$$

The bar over the term in parentheses indicates that the entire term is averaged. The term ε is the turbulence dissipation rate

$$\varepsilon = \frac{C(\mathrm{k})^{3/2}}{l_\varepsilon} \tag{G14}$$

where

l_ε = dissipation length;
C = constant.

In addition to the above constant, there are several others, and the values in the 1974 paper by Launder and Spalding are almost the same ones used for most applications today. For a discussion about extension of the k-ε model to compressible flow and a general presentation about the mathematics of CFD to fire applications, the reader is referred to Kumar (1983).

3. Application of Software

Software for CFD applications falls into one of the following groups: (1) pre-processing, (2) processing, and (3) post-processing. Not all CFD packages have all these software groups, but they are available in all of the large commercial packages. Pre-processing software helps the user generate the grid, specify the boundary conditions, and define other input parameters. For geometries that are somewhat complicated, grid generation capabilities can save significant amounts of user time.

The processing software simulates the flow, but often the user can enter data in a batch file read directly by the processing software to further define the simulation. Some CFD codes allow the user to write FORTRAN routines that become part of the processing software. Such routines can define an unusual boundary condition or the performance of a detector. Processor software generates files of computer generated data.

Post-processing software is used for graphic display of data from the files. This display can vary from simple 2-D black and white contour plots to 3-d color movies where the view can move around the flow field.

For a three dimensional simulation, it is not unusual to divide the space of interest into about 50,000 cells, and some applications have many times more. For each cell pressure, density, temperature, three velocity components, and a number turbulence modeling variables are calculated several times for each second of simulated time. To reduce the size of files, data is not stored for every time step calculated, in some cases it is stored every 10 seconds of simulated time. If a fire simulation has 50,000 cells and saves 10 variables per cell for 10 seconds simulated, 20 minutes of simulated fire results in the generation of a file of over 60 million numbers. CFD is probably unique among engineering applications in regard to the challenges of output data.

4. Example Analyses

An example fire application of CFD is the NIST analysis of flame blow-down at a Navy fire fighter training facility (Forney and Davis 1992). The facility was used recreate the effects of jet pool fires on the deck of a ship. A section of "deck" surface was built of steel grating below which there were computer controlled propane burners that simulated the fires. When there was little or no wind, the flames would be 2.5 to 3 m (8 to 10 ft) high. However, under moderate winds, the flames would be blown down into the space below the grating. CFD simulations were made to evaluate possible alternative solutions to this problem, and arrive at a solution. One alternative was a wall intended to shield the facility, and the performance of this is shown in figure G2. The wall resulted in flame flow toward the wall (figure G2), but it did not prevent flame blow-down. The solution consisted of a combination of a fence in place of the wall plus pressurization of space under the grating. When installed, this solution qualitatively preformed as predicted.

Another example is the project to evaluate the effects of flat beamed ceilings on detector and sprinkler response (Forney, Davis and Klote 1992; Forney, Bukowski and Davis 1993). Figure G3 shows the temperature contours in a vertical plane perpendicular to ceiling beams. Comparison of simulated and experimental temperatures indicates the extent to which CFD analysis can be expected to predict flow under ceilings (figure G4). Twenty cases were run for various fire growth rates, beam depths, beam spacings and ceiling heights. These data were used to develop recommendations on placing sensors in rooms with beamed ceilings.

Comparisons of room fire data with CFD simulations have been conducted by Davis, Forney and Klote (1991) and Morita and Hirota (1989). Waters (1989) conducted a CFD simulation for design purposes of a large volume space at the Stansted Terminal in the United Kingdom. A CFD analysis was made as part of the fire reconstruction for the fire at the King's Cross train station in London England (Simcox, Wilkes and Jones 1988, 1989).

5. Considerations about CFD

As the examples above show, CFD modeling is capable of simulating levels of flow detail that are impossible with zone modeling and often more expensive with physical modeling. Because CFD is based

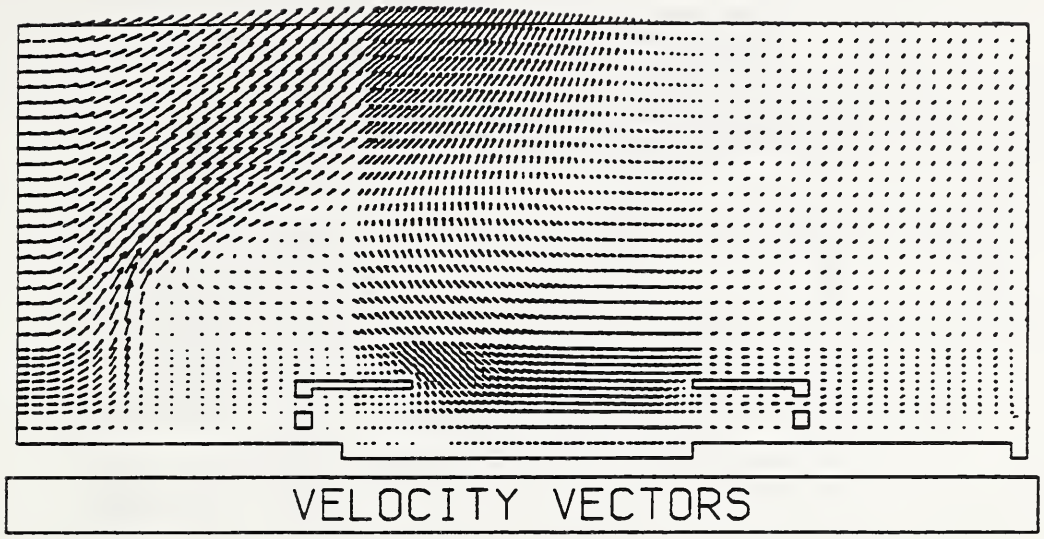

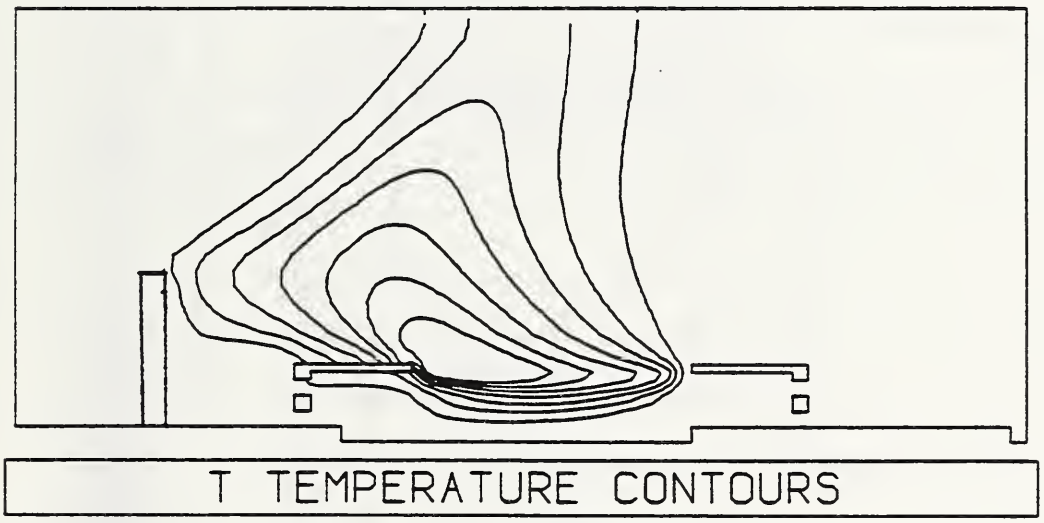

Figure G2 CFD simulated velocity and temperature contours of flame blow-down at Navy fire fighter training facility

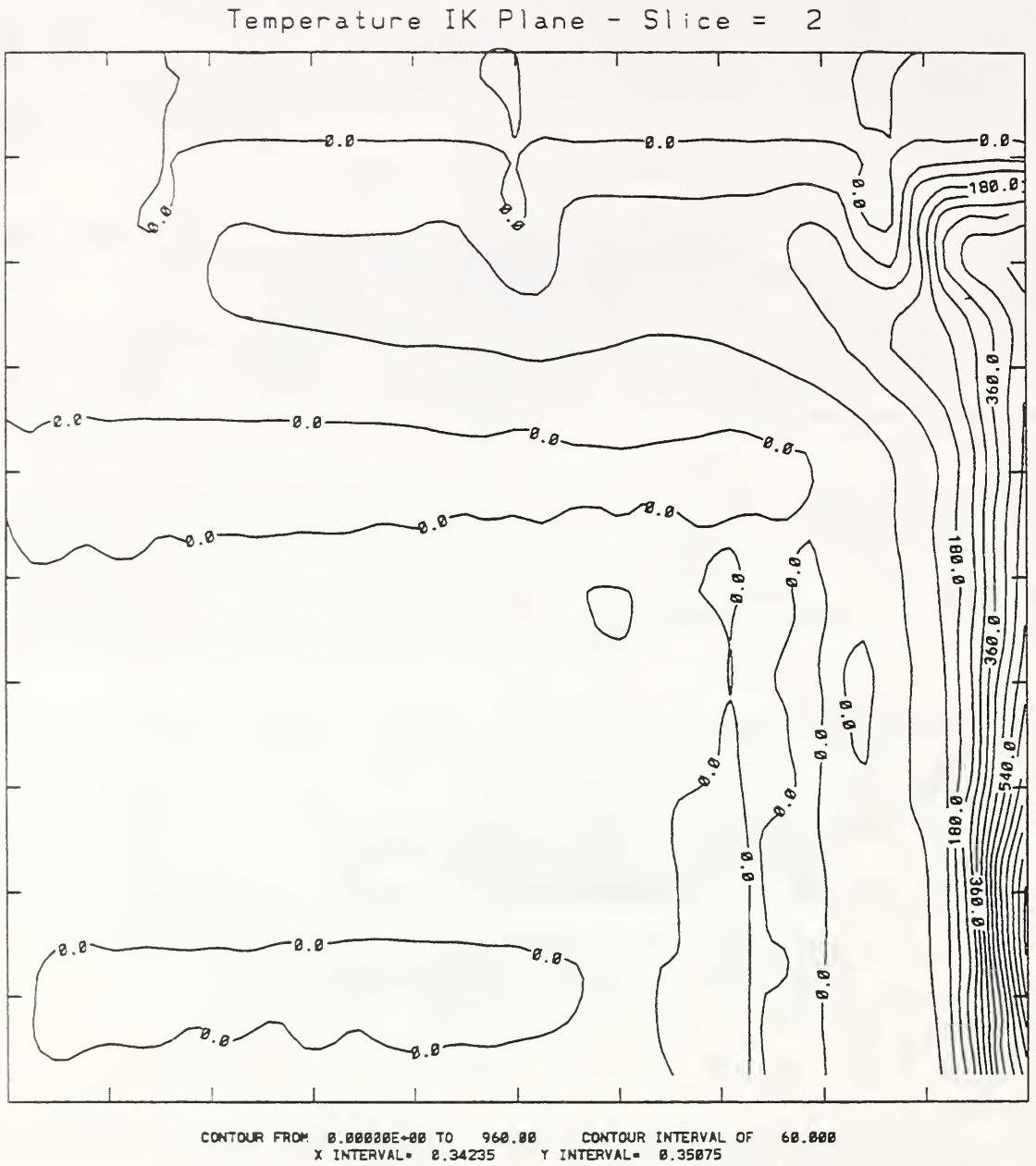

Figure G3 CFD simulated temperature rise (K) in a vertical plane containing fire and perpendicular to ceiling beams

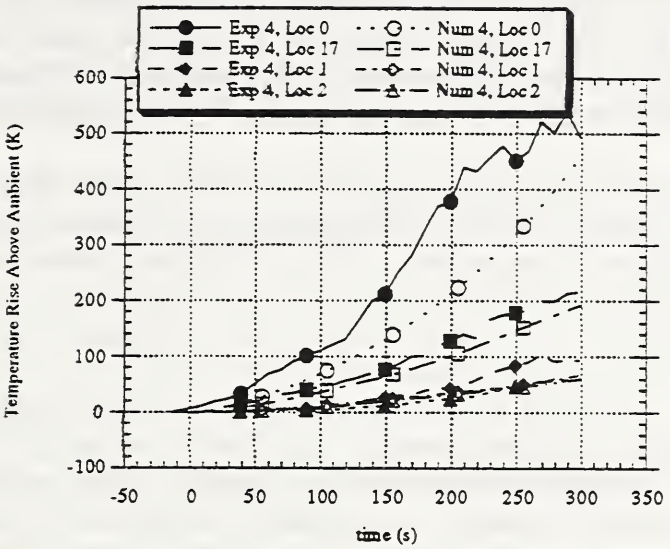

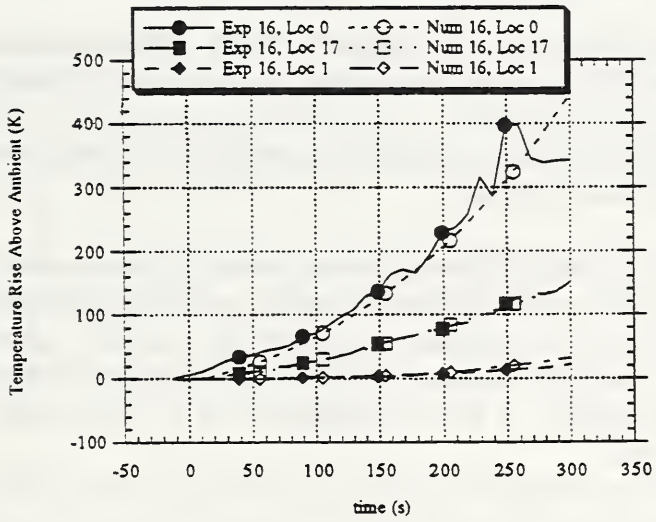

Figure G4 Comparison of CFD simulated temperatures and experimental data for flow under a beamed ceiling

on approximate turbulence models and requires a high level of expertise, unusual care needs to be taken to assure the applicability of the results.

Generation of grids that allow realistic simulations in a practical time frame requires experience. For example, in the Navy blow-down study, a smaller grid spacing was used near the flame (figure G2). The more complicated ceiling project required a more complex grid arrangement (not shown). Much more complex gridding is required for more complex geometries, for example smoke flow in aircraft cabins (De Souza, Yang and Lloyd 1985; Galea and Markatos 1989; Yang et al. 1983 and 1984). CFD users need to exercise caution, because inappropriate selection of gridding will lead to simulation errors.

Simpler simulations not only require less time to compute, but they are less likely to have convergence failures. A simpler approach is especially important when a project consists of simulations for a large number of cases as did the beamed ceiling project. Ideally simulations should have the lowest level of simplicity that results in acceptable results. However, it is not possible to know ahead of time what level of complexity is sufficient.

One approach to the issue of simulation complexity, that has been used at NIST with success, is to systematically go from the simple to the more complex. For example, an analysis may start with course gridding and be modeled as Boussinesq flow without heat transfer. Upon successful simulation, the complexity is then increased perhaps by going to compressible flow. Increased complexity would include closer grid spacing and addition of some heat transfer. Eventually, increasing the level of complexity will have little impact on the results. This point is clearly the lowest level of simplicity that results in acceptable results. The King's Cross analysis is a good example of systematically increasing complexity.

Considering that application of CFD is an art and that the turbulence models are approximate, simulations need to compared to experimental data. This is especially true of new applications, and it is why many of the projects above included such comparisons. If a simulation is similar in most respects to others that have been experimentally verified, further experimental verification is not necessary. This was the approach taken with the beamed ceiling project.

A discussion of practical concerns with CFD simulations should include mention of the times involved to conduct a CFD analysis. Such an analysis should consist on many simulations at various levels of detail. Run time for simulations like the ones discussed above are generally measured in days. Analysis of the simulated fire data also takes days. Generally, simulations are made at the same time as the output from earlier runs are being analyzed. It is not uncommon for a CFD analysis consisting of many simulations to take several months.

6. References

Abbott, M.B. and Basco, D.R. 1989. Computational Fluid Dynamics: An Introduction for Engineers, Wiley, New York, NY.

Anderson, D.A., Tannehill J.C. and Pletcher, R.H. 1984. Computational Fluid Mechanics and Heat Transfer, Hemisphere, New York, NY.

Aris, R. 1962. Vectors, Tensors, and the Basic Equations of Fluid Mechanics, Dover, New York, NY.

Davis, W.D., Forney, G.P. and Klote, J.H. 1991. Field Modeling of Room Fires, National Institute of Standards and Technology, NISTIR 4673.

De Souza, B.P., Yang, K.T. and Lloyd, J.R. 1985. Numerical Simulations of the Effect of Floor and Ceiling Venting on Fire and Smoke Spread in Aircraft Cabins. National Bureau of Standards, Gaithersburg, MD. NBS-GCR-84-479.

Forney, G.P., Bukowski, R.W., Davis W.D. 1993. Field Modeling: Effects of Flat Beamed Ceilings on Detector and Sprinkler Response, National Fire Protection Research Foundation, Quincy, MA.

Forney, G.P. and Davis, W.D. 1992. Analyzing Strategies for Elimination of Flame Blow-down Occurring in the Navy's 19F4 Fire Fighting Trainer, National Institute of Standards and Technology, NISTIR 4825.

Forney G.P., Davis, W.D. and Klote, J.H. 1992. Simulating the Effect of Beamed Ceilings on Smoke Flow, Part I. Comparison of Numerical and Experimental Results, National Institute of Standards and Technology, NISTIR 4994.

Friedman, R. 1992. An International Survey of Computer Models for Fire and Smoke, Journal of Fire Protection Engineering, Vol 4, No 3, pp 81-92.

Galea, E.R. and Markatos, N.C. 1989. Modelling of Aircraft Cabin Fires, Fire Safety Science - Proceedings of the Second International Symposium, pp 801-810.

Harlow, F.H. and Nakayama, P.I. 1968. Transport of Turbulence Energy Decay Rate, Los Alamos Scientific Laboratory of the University of California, Los Alamos, NM.

Hirsch, C. 1988. Numerical Computation of Internal and External Flows, Vol 1: Fundamentals of Numerical Discretization, Wiley, New York, NY.

Hirsch, C. 1990. Numerical Computation of Internal and External Flows, Vol 2: Computational Methods for Inviscid and Viscous Flows, Wiley, New York, NY.

Hoffmann, K.A. 1989. Computational Fluid Dynamics for Engineers, Engineering Education System, Austin, TX.

Kumar, S. 1983. Mathematical Modelling of Natural Convection in Fire - A State of the Art Review of the Field Modelling of Variable Density Turbulent Flow, Fire and Materials, Vol 7, No 1, pp 1-24.

Launder, B.E. and Spalding, D.B. 1974. The Numerical Computation of Turbulent Flows, Computer Methods in Applied Mechanics and Engineering, Vol 3, pp 269-289.

Markatos, N.C. 1986. The Mathematical Modelling of Turbulent Flows, Applied Mathematical Modeling, Vol 10, no 3, pp 190-220.

Morita, M. and Hirota, M. 1989. Numerical Analysis and Experiments of Convective Heat Flow in Fire Compartments, Fire Science and Technology, Vol 9, No 1, pp 11-24.

Schetz, J.A. 1993. Boundary Layer Analysis, Prentice Hall, Englewood Cliffs, NJ.

Schlichting, H. 1960. Boundary Layer Theory, 4th ed., Kestin, J. Translator, McGraw, New York, NY.

Sherman, F.S. 1990. Viscous Flow, McGraw, New York, NY.

Simcox, S., Wilkes, N.S. and Jones, I.P. 1988. Fire at King's Cross Underground Station, 18th November 1987: Numerical Simulation of the Buoyant Flow and Heat Transfer, Harwell Laboratory, UK.

Simcox, S., Wilkes, N.S. and Jones, I.P. 1989. Computer Simulation of the Flows of Hot Gases From the Fires at King's Cross Underground Station, Institution of Mechanical Engineers (IMechE) King's Cross Underground Fire: Fire Dynamics and the Organization of Safety, London, UK, pp 19-25.

Waters, R.A. 1989. Stansted Terminal Building and Early Atrium Studies, Journal of Fire Protection Engineering, Vol 1, No 2, pp. 63-76.

White, F.M. 1974. Viscous Fluid Flow, McGraw, New York, NY.

Yang, K.T., Lloyd, J.R., Kanury, A.M. and Satoh, K. 1984. Modeling of Turbulent Buoyant Flows in Aircraft Cabins. Combustion Science and Technology, Vol 39, No 1, 107-118.

Yang, K.T., Lloyd, J.R., Kanury, A.M. and Satoh, K. 1983. Numerical Calculations of Turbulent Buoyant Flow in Aircraft Cabins. Report. Notre Dame Univ.

Appendix H Considerations of the Steady Plume

The theoretical plume equations presented in the text are for steady flow plumes. For a steady flow process, (1) the control volume does not move (relative to smoke reference frame), (2) the state of mass at each point in the control volume does not vary with time, and (3) the mass flux and mass state at each discrete area of flow on the control volume surface do not vary with time. Because the state of mass does at each point not very, these processes are also referred to as steady state processes.

In the idealized plume models, the properties of mass at each point in the plume are constant with time, even though the properties of a given elemental mass of gas vary as it flows through the plume. As already stated, plumes are in constant and often wandering motion. In laboratory experiments, time averaged measurements of temperature and velocity are made. The theoretical plume models might be thought of as equilibrium conditions about which the properties fluctuate.

Generally, implementation of plume models in computer fire models consists of algebraic equations (such as those above) that are used to calculate the plume flow mass at an elevated temperature to the upper layer. This mass is added to the upper layer at the instant that heat is released form the fire. This is consistent with the steady plume. When the time for smoke travel to the upper layer is small in comparison to the fire event, this instantaneous mass transfer assumption is appropriate. Zone fire models were developed for room fires, and the instantaneous mass transfer assumption is basic to zone fire models.

The plume travel time can be considered for a plume in early development or for a developed plume. The developed plume reaches that atrium ceiling and can be approximated by the plume equations. In the early stages, a plume develops above the fire and starts to flow upward. As the plume rises, it entrains air and its buoyancy decreases. In the early stages of a growing atrium fire, the plume can not be expected to be sufficiently buoyant to reach the ceiling. The time lag for smoke to reach the atrium ceiling may be significant. The presence of a pre-stratified hot layer of air under the ceiling extends this lag time significantly. Further research is needed to study the lag time for smoke from a developing fire to reach the atrium ceiling.

For a developed plume in an atrium with a ceiling height of 100 m (330 ft), the travel time estimated from equations (7, 8, 11, 12 and 14) is listed below.

Heat Release Rate, Q		Plume Travel Time to Reach 100 m (330 ft) Ceiling, s
kW	Btu/s	
2,000	1,900	100
5,000	4,740	70
25,000	23,700	40

One meaning of the fire event time is the evacuation time. If the building were an atrium office building, the evacuation time is roughly 2 minutes per floor. For a floor-to-ceiling height of 3 m (10 ft), the

atrium building would have an evacuation time of about a hour. The plume travel times above are insignificant in comparison with the building evacuation time.

The evacuation time could also be taken as the time for decision making and travel to an exit stairwell on the same floor. This floor evacuation time is on the order of 5 minutes. The plume travel time cannot be considered insignificant in comparison with the floor evacuation time. However, the zone fire models neglect the plume travel time, so that the error is conservative in that people would have more time for evacuation than a zone model would predict.

In conclusion, the plume travel time is not important in atrium applications for developed plumes, but research is needed to study the lag time for smoke from a developing fire to reach the atrium ceiling.

NIST-114
(REV. 6-93)
ADMAN 4.09

U.S. DEPARTMENT OF COMMERCE
NATIONAL INSTITUTE OF STANDARDS AND TECHNOLOGY

MANUSCRIPT REVIEW AND APPROVAL

(ERB USE ONLY)

ERB CONTROL NUMBER	DIVISION
PUBLICATION REPORT NUMBER	**CATEGORY CODE**
NISTIR 5516	
PUBLICATION DATE	**NUMBER PRINTED PAGES**
October 1994	

INSTRUCTIONS: ATTACH ORIGINAL OF THIS FORM TO ONE (1) COPY OF MANUSCRIPT AND SEND TO THE SECRETARY, APPROPRIATE EDITORIAL REVIEW BOARD.

TITLE AND SUBTITLE (CITE IN FULL)

Methods of Predicting Smoke Movement in Atria and Other Large Spaces

CONTRACT OR GRANT NUMBER

TYPE OF REPORT AND/OR PERIOD COVERED

AUTHOR(S) (LAST NAME, FIRST INITIAL, SECOND INITIAL)

Klote, John H.

PERFORMING ORGANIZATION (CHECK (X) ONE BOX)

[X] NIST/GAITHERSBURG
[ ] NIST/BOULDER
[ ] JILA/BOULDER

LABORATORY AND DIVISION NAMES (FIRST NIST AUTHOR ONLY)

Building and Fire Research, Fire Safety Engineering Division - 864

SPONSORING ORGANIZATION NAME AND COMPLETE ADDRESS (STREET, CITY, STATE, ZIP)

PROPOSED FOR NIST PUBLICATION

[ ]	JOURNAL OF RESEARCH (NIST JRES)	[ ]	MONOGRAPH (NIST MN)	[ ]	LETTER CIRCULAR
[ ]	J. PHYS. & CHEM. REF. DATA (JPCRD)	[ ]	NATL. STD. REF. DATA SERIES (NIST NSRDS)	[ ]	BUILDING SCIENCE SERIES
[ ]	HANDBOOK (NIST HB)	[ ]	FEDERAL INF. PROCESS. STDS. (NIST FIPS)	[ ]	PRODUCT STANDARDS
[ ]	SPECIAL PUBLICATION (NIST SP)	[ ]	LIST OF PUBLICATIONS (NIST LP)	[ ]	OTHER _____
[ ]	TECHNICAL NOTE (NIST TN)	[X]	NIST INTERAGENCY/INTERNAL REPORT (NISTIR)		

PROPOSED FOR NON-NIST PUBLICATION (CITE FULLY) [X] U.S. [ ] FOREIGN

PUBLISHING MEDIUM

[X] PAPER [ ] CD-ROM
[ ] DISKETTE (SPECIFY) _____
[ ] OTHER (SPECIFY)

SUPPLEMENTARY NOTES

ABSTRACT (A 2000-CHARACTER OR LESS FACTUAL SUMMARY OF MOST SIGNIFICANT INFORMATION. IF DOCUMENT INCLUDES A SIGNIFICANT BIBLIOGRAPHY OR LITERATURE SURVEY, CITE IT HERE. SPELL OUT ACRONYMS ON FIRST REFERENCE.) (CONTINUE ON SEPARATE PAGE, IF NECESSARY.)

In recent years, building with atria has become commonplace. Other spaces including enclosed shopping malls, arcades, sports arenas and airplane hangers also have large volumes, and the methods of this paper are also applicable to these spaces. This paper presents information that can be used for predicting smoke movement for design of atrium smoke management systems. The basic approach used in many codes consists of a collection of algebraic equations for design analysis. This approach and the physical concepts behind it are discussed including atrium smoke management system limitations. For applications for which the basic approach is inappropriate, computational fluid dynamics (CFD) and physical modeling can be applied. Research is needed concerning (1) the depth of smoke layer required to prevent atrium exhaust from pulling air from the lower layer and (2) the use of airflow for smoke control between the atrium and spaces opening onto the atrium.

KEY WORDS (MAXIMUM OF 9; 28 CHARACTERS AND SPACES EACH; SEPARATE WITH SEMICOLONS; ALPHABETIC ORDER; CAPITALIZE ONLY PROPER NAMES)

atriums; building fires; fire models; fire plumes; fire research; plumes; scale models; smoke control

AVAILABILITY

[X] UNLIMITED [ ] FOR OFFICIAL DISTRIBUTION - DO NOT RELEASE TO NTIS
[ ] ORDER FROM SUPERINTENDENT OF DOCUMENTS, U.S. GPO, WASHINGTON, DC 20402
[ ] ORDER FROM NTIS, SPRINGFIELD, VA 22161

NOTE TO AUTHOR(S): IF YOU DO NOT WISH THIS MANUSCRIPT ANNOUNCED BEFORE PUBLICATION, PLEASE CHECK HERE. [ ]

ELECTRONIC FORM